Soil Characterization Utilizing GPR Technique

SOIL CHARACTERIZATION UTILIZING GPR TECHNIQUE

by

Fateh Tamam Al Kej

A Thesis Presented to the Faculty of the
American University of Sharjah
College of Engineering
in Partial Fulfillment
of the Requirements
for the Degree of

Master of Science
in Civil Engineering

Sharjah, United Arab Emirates

Fall 2017

Approval Signatures

We, the undersigned, approve the Master's Thesis of Fateh Tamam Alkej

Thesis Title: Soil Characterization Utilizing GPR Technique

Signature	**Date of Signature** (dd/mm/yyyy)
____________________	____________
Dr. Magdi El-Emam Associate Professor, Department of Civil Engineering Thesis Advisor	
____________________	____________
Dr. Sherif Yehia Professor, Department of Civil Engineering Thesis Co-Advisor	
____________________	____________
Dr. Nasser Qaddoumi Professor and Department Head of Electrical Engineering Thesis Co-Advisor	
____________________	____________
Dr. Mousa Attom Professor, Department of Civil Engineering Thesis Committee Member	
____________________	____________
Dr. Amer Samir Zakaria Assistant Professor, Department of Electrical Engineering Thesis Committee Member	
____________________	____________
Dr. Robert John Houghtalen Head, Department of Civil Engineering	
____________________	____________
Dr. Ghaleb Husseini Associate Dean, College of Engineering	
____________________	____________
Dr. Richard T. Schoephoerster Dean, College of Engineering	
____________________	____________
Dr. Mohamed El-Tarhuni Vice Provost for Graduate Studies	

Acknowledgments

I am very grateful to ALLAH the Almighty God for His endless guidance and support during all my life. My thanks also go to my family. Words are not enough to thank them for being always by my side, supporting and helping me in every action, keeping me focused, and raising me up during my failures. In addition, I would like to thank my supervisors, Dr. Magdi El-Emam, Dr. Sherif Yehia, and Dr. Nasser Qaddoumi, for sharing their knowledge and guiding me through this research program at every stage. Without their experience, encouragement and personal support this thesis would not have been possible. This work cannot also go without thanking Mr. Aqeel Ahmed, Instructor of Practice (geotechnical lab) at the American University of Sharjah (AUS), for the help provided during the experimental part of this work. Furthermore, I am grateful for American University of Sharjah for giving me a Graduate Teaching Assistantship and funding my research. Finally, I want to thank my friends, Firas Al-Otaibi, Tariq Alsayed, and Moncef Khouchane for being by my side and helping me during this research.

Abstract

Engineering properties of soil, such as shear strength parameters, water content, degree of saturation, and permeability are essential for safe and economic design of any structure involving soil structure interactions. The invasive conventional testing methods for determining soil properties usually commence by extracting soil samples from different depths, testing them in the geotechnical lab, and comparing lab results with field test results for verification. These steps and procedures are time consuming and highly expensive, which is expected to affect the construction time and cost of any project. Noninvasive, nondestructive techniques represent a suitable alternative to the time consuming and expensive conventional site investigation procedures. However, to practically implement nondestructive techniques with acceptable confidence, a database of correlation equations need to be acquired and well established. The work conducted in this research is a major step on a long term research project to build such database to correlate Ground Penetrating Radar (GPR) output to different soil engineering properties. GPR is an attractive tool for subsurface inspection and quality control on construction projects due to its time saving, economy, and noninvasiveness. In the current research, a group of index tests has been conducted in order to relate soil resistivity to water contents for different sandy soils. In addition, laboratory direct shear tests were conducted to measure the soil shear strength parameters at different water contents and different particle distributions. The soil dielectric constant at different water contents and different gradations is measured using the GPR technique. Index test results indicate that soil electrical resistivity is inversely proportional with the water content and compaction effort. In addition, electrical resistivity of sandy soil increases as both particle size and void ratio increase. Finally, soil resistivity increases with clay content up to certain limit and decreases thereafter. GPR test results show that, the soil dielectric constant is directly proportional to water content and inversely proportional to compaction effort. Results of index tests, lab tests, and GPR scanning test output are analyzed and correlated using regression analyses, and a 3-dimensional yet practical graph is produced for the soil types considered in this study. The proposed graph can be used to extract the soil friction angle from a rapid GPR in site scanning of any soil with similar properties.

Search Terms: ***GPR, Resistivity, Dielectric constant, Friction angle, Water content***

Table of Contents

List of Figures

List of Tables

Chapter 1: Introduction

1.1 General

Soil properties such as unit weight, permeability, porosity, water content, friction angle, and gradation are examples of significant parameters that are needed in the design and construction stage of any project that is in contact with the soil. Most of these parameters can be measured in the lab as well as in-situ. For example, soil friction angle can be measured in the lab using either triaxial or direct shear tests. It can also be measured in-situ using Standard Penetration Test (SPT), or Cone Penetration Tests (CPT). However, lab tests are time consuming and require soil samples which might not represent the soil in-situ. In-situ tests are based on correlation equations which fit well with soil located with the data base these correlations developed for.

Although all these parameters are not independent variables, this research focuses on a significant property which is the friction angle. The friction angle of the soil is important to be known because it greatly affects the bearing capacity of the soil. The friction angle is affected by parameters such as the dry density, liquefaction, sphericity, surcharge pressure, particle size, and gradation. Due to advancement in technology, it is now affordable to measure some soil's properties utilizing nondestructive techniques. Thus, an alternative way to predict the angle of friction is to measure it using nondestructive methods in the site which it could be related to. Some nondestructive tests, such as using an infrared camera, ground penetrating radar, and seismic refraction can be helpful. These tests have several advantages over lab techniques. For example, nondestructive techniques measure the properties directly and without disturbing the nature of the soil. They also save time and are more cost efficient in comparison to lab techniques. Therefore, this research focuses on measuring the angle of fiction of soil using ground penetrating radar and geophysical tests.

1.2 Ground Penetrating Radar (GPR)

Ground penetrating radar (GPR) is a noninvasive geophysical technique that detects electrical discontinuities in the shallow subsurface (<50 m). It is an electromagnetic (EM) technique designed to locate objects or interfaces buried underneath the ground surface, or located within a visually opaque medium. It does this by generation, transmission, propagation, reflection and reception of discrete pulses of high-frequency electromagnetic energy. This is accomplished by employing an antenna to transmit and receive EM signals, a transmitter and a receiver, and a processor that are contained within a sealed enclosure. Additionally, the system includes a battery, a control processor and a display unit. The operation of GPR is summarized as follows. The Radar radiates electromagnetic energy in the form of repetitive pulses that are launched from the antenna to the surface of the ground. Since ground is not made of a perfect conductor, some of the EM energy will propagate through the upper layer. Each material is characterized by a property known as the dielectric constant. Dielectric constant is a quantity for measuring the ability of a substance to store electrical energy in an electric field. EM signals are very sensitive to variations in the dielectric constant and as they encounter any new object or ground layer with a different dielectric constant, part of the energy will be reflected. The magnitude of the signal that gets reflected depends on the difference between the dielectric constants of the original layer and the new object or layer, and their shape and dimensions. Additionally, microwave signals are known to travel at speed of light in air; however, they travel at different speeds in different materials. As the dielectric constant increases, wave velocity decreases, and the time at which the reflected signal arrives back at the receiver changes. Turesson (2006) [1] approximates propagation velocity (V) of an electromagnetic wave in a medium by Eq 1.

$$V = \frac{C}{\sqrt{K}} \text{..Eq 1.}$$

Where K is the dielectric constant, and C is the velocity of electromagnetic wave in free space (3×10^8 m/s). Thus, by using the magnitude to the reflections associated with traveling from one medium to another and the variation of wave speed, information about the properties of the structure could be obtained. The reflected signals, also known as echo, are picked up by the antenna and are then amplified by the receiver. To make a decision on the electrical and mechanical properties of the different layers of a structure, the signals are then fed into the processing unit where a display unit will show the output. Table 1 summarizes the applications, advantages, and limitations of GPR.

Table 1: Applications, advantages and limitations of using GPR

Applications	Advantages	Limitations
• Subsurface features of soil layers which include depths of layers, existence of organic carbon content, water content, porosity, and density. • Electrical properties of soil. • Utility and buried objects. • Defects in concrete structures.	• Nondestructive techniqe and is relatively fast. • Produces large quantities of continous high resolution subsurface data. • Economical (saves time and is more prodictive) compared to conventional methods, and there are less chances to overlook subsurface features.	• GPR can not be used with soils that have the following features: 1. High electrical conductivity 2. Saturated soil

1.3 Problem Statement

Internal friction angle, unit weight, water content, and void ratio/porosity are soil properties that are required for any geotechnical work. Friction angle is typically obtained from laboratory tests, such as Triaxial or Direct shear tests. Unit weight and water content are measured in-situ using sand cone, which is time consuming and not as accurate as interpreted. These tests are conducted on extracted samples that could be disturbed during the sampling process, or in reconstituted samples which might not represent the real soil in-site. Void ratio or porosity is an important soil property that affects several parameters, including permeability. Void ratio is usually calculated indirectly using the well-known phase relation, unit weight and soil specific gravity. Measuring the soil specific gravity is somewhat cumbersome and could lead to major errors, which in turn affects the calculated void ratio and porosity.

To avoid disadvantages and limitations of the conventional lab and in-site tests, nondestructive/noninvasive techniques attract the attention of geotechnical research workers. The main objective of the current research is to study the implementation of Ground Penetration Radar (GPR) in predicting the major soil properties of sandy soil. Soil parameters that are of interest to geotechnical engineers are: soil friction angle (ϕ), water content (w), and void ratio (e). The final goal of this research is to use the GPR together with variation of soil conductivity to predict the angle of friction which is needed for designing any geotechnical project.

To achieve this goal, different types of sandy soil are subjected to intensive laboratory tests, including sieve analysis, Direct Shear tests, and Standard Proctor tests. The main objective of these index tests is to study the variation of the soil conductivity with variation of these soil parameters. In addition, a scaled test setup is constructed in the geotechnical lab at the American University of Sharjah (AUS) to test the variation of these parameters in a large scale using the AUS GPR facility. Results of this research facilitate site investigation phase for any geotechnical project and reduce the cost and time required in site investigation.

1.4 Research Objectives

Based on the problem statement explained above, this research aims to:

1. Quantify the variation of soil conductivity with friction angle and with moisture contents and void ratio for different soil gradation with different compaction efforts.
2. Quantify the variation of soil friction angle, moisture contents, void ratio for different soil gradation.
3. Study the effect of adding clay to sandy soil on conductivity tests for the soil by varying the moisture content.
4. Construct a test setup that can be used together with different soil and GPR to deduce different soil properties from GPR images after suitable imaging processing.
5. Develop analytical models that relate friction angle with soil conductivity.
6. Build a suitable database that could be used by geotechnical engineers to facilitate soil investigation and parameters determinations.

1.5 Significance of the Research

The current research is particularly significant for the following reasons:

1. It is considered a new research trend in soil investigation, nondestructive testing, and geotechnical field.
2. It explored noninvasive Ground Penetration Radar technique to assess its feasibility to be used commercially in geotechnical engineering.
3. The results of this research help reduce cost and time of soil investigation which will be reflected positively on design, construction, and budget of different projects
4. The results of this study also lead to a correlation between data obtained from the GPR and that obtained from the current conventional lab and field soil tests.
5. This research sets the bases for future research in the field of using nondestructive techniques for measuring properties of soil.

1.6 Thesis Organization

This thesis is organized into six chapters. The first chapter provides background information about the problem being addressed and introduces the GPR as a nondestructive technique that is used in order to meet the objectives of the study. The second chapter provides a review of the literature on the GPR and geotechnical applications. Moreover, the third chapter discusses the methodology used in this research, and the results are reported and discussed in the fourth chapter. Chapter five implements and analyzes the research results obtained. Finally, chapter six concludes and summarizes the research. It also sets the basics for future work in the GPR research area.

Chapter 2: Literature Review

2.1 Soil Investigation

Determining soil characteristics and properties is an important step to understand its behavior and performance. Different soil properties can be determined by extracting both disturbed and undisturbed samples from the site, and testing them in the lab. Although this procedure is commonly used, it has disadvantage of altering the actual properties of the soil sample due to some disturbances. Even though test conditions could be ideal in terms of temperature and humidity control, these tests are still unable to reflect the in-site condition from the behavior of small soil sample. Therefore, a number of studies have been conducted in order to demonstrate the ability of measuring different soil properties in site using the noninvasive technique of Ground Penetration Radar (GPR). This technique helps to save cost and time compared to both lab and in-site invasive tests methods. Examples of other nondestructive, noninvasive soil measuring techniques are: ground infrared camera, and geophysical methods. Table 2 illustrates some efforts of using nondestructive methods for determining soils properties.

Table 2: Nondestructive techniques used for measuring soil's properties

Authors	Equipment Used	Limitations	Results
Lambot, Slob, Vanclooster, and Vereecken (2006) [2]	GPR "Ultra wide band Continuous wave stepped frequency of ground monostatic GPR"	Inhomogeneous and continuously variable dielectric media.	* Air entry value parameter (α) and pore size distribution parameter (n) are negatively correlated. * Saturated hydraulic conductivity (Ks) is positively correlated with other parameters. * Tortuosity (λ) is quite sensitive.
Turesson (2006) [1]	GPR "Antenna were 2m apart with frequency of 50 MHz"	* Absence of several electromagnetically contrasting layers. * The material should be more or less horizontal to	Water content and porosity can be measured in sand.

		satisfy the equations used.	
Luong (2007) [3]	Infrared thermography "A scanning camera that utilizes an infrared detector system that detects radiated energy and converts it to detailed real-time thermal picture.		Infrared thermography can be used in fine sand to find energy dissipation.
Bouten, Heuvelink, Huisman, and Snepvangers (2002) [4]	GPR "Pulse EKKO™ 1000 GPR with 200V transmitters. Antennas with center frequency 225MH, antennas were separated by 1.54m.	Small scale studies in SWC due to high water content and high sprinkling intensity of the small scale structures.	* GPR measurements resulted in lower variations in SWC. * GPR can be used for large fields to find SWC.
Muñoz, and Kravchenko (2011) [5]	* NIR with spectrophotometer * Light Detecting and ranging (LIDAR) with at least 15.2cm and vertical accuracy 100cm.		NIR can be used to determine the carbon in the soil.
Kodaira, and Shibusawa(2013) [6]	NIR (305-1700nm)	Weak signals and noise	* PH, N-a, P-a, were accurate. * EC, N-n was of poor accuracy. *CEC, C-t is accurate.
Pozdnyakov, Pozdnyakova, and Zhang (2001) [7]	* EP (electrical profiling) * VES (vertical electrical surrounding) * GPR	It works for near surface only.	The four methods were powerful to investigate hydrology and soil properties.

	* EM (electromagnetic induction)		
Bouma, Heijs, Lange, and Schoute (1995) [8]	Computed Tomography (CT)		Macroporosity and water content (WC) can be quantified from CT images.
Garcia, He, Hernandez, Huang, and Song (2007) [9]	NIR		NIR is an effective technique to evaluate N,OM, PH.
Or, and Serbin (2004) [10]	GPR, and 30 AGG monostatic horn antenna generate a monostatic signal with frequency between 50MHz to 2.5GHz.	Excessive noise (ex: irrigation)	GPR measurements show good agreement with gravimetric measurement of water content (WC).
Janik, McBratney, Rossel, Skjemstad, and Walvoort (2006) [11]	* UV-VIS-NIR with a diffuse accessory DRA-CA-SOD * Biorad FTS 175		MIR produced more accurate results for predictions of PH, LR, OC, CEC, clay, silt, sand content, P, and EC.
Noborio (2001) [12]	Time Domain Reflectometry (TDR)		Several TDR techniques (using 2 probes, 3 probes, etc.) were useful for predicting WC&EC.

2.2 Nondestructive techniques for Soil

Bouten et al. (2002) [4] used the GPR technique in mapping soil water content. In addition, they compare the results from GPR with those obtained using time domain reflectometry (TDR). Their study indicates that the GPR technique is able to determine the water content in the soil as illustrated in Figure 1. The researchers conclude that the GPR is more suitable than TDR in mapping soil water content for its large scale features. This is showed by the ability of the GPR to collect more measurements with the same effort compared to TDR.

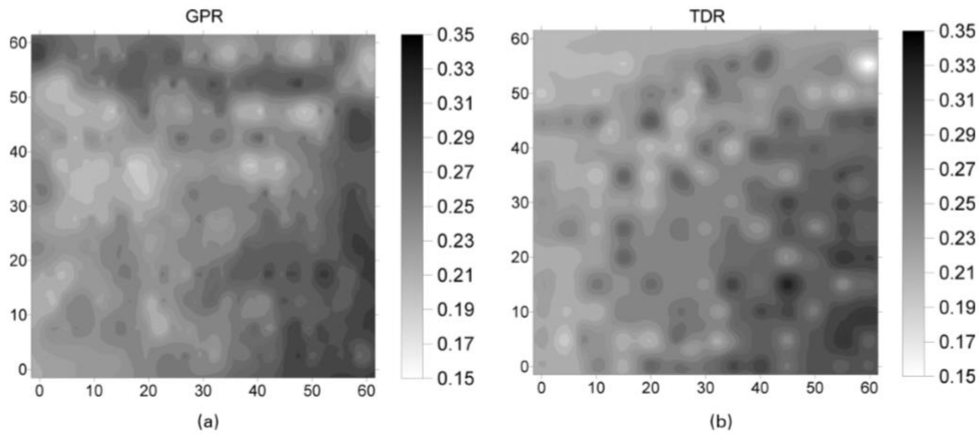

Figure 1: Interpolated maps of initial soil water content (m^3 m^{-3}) before irrigation, measured with GPR and TDR. (Bouten et al., 2002) [4]

Or, and Serbin (2004) [10] conducted a study to assess the implementation of GPR with directional horn antenna for measuring soil water content. Their study was performed on a sandy soil, aiming to verify the results obtained from the GPR with those obtained using both TDR and gravimetric methods. Moreover, they also investigated the effect that the soil temperature has on the GPR resistivity. The researchers find out that GPR measurements of water content for the top 1 cm layer were in agreement with the gravimetric measurements. Their results for GPR measurements of volumetric water content are shown in Figure 2.

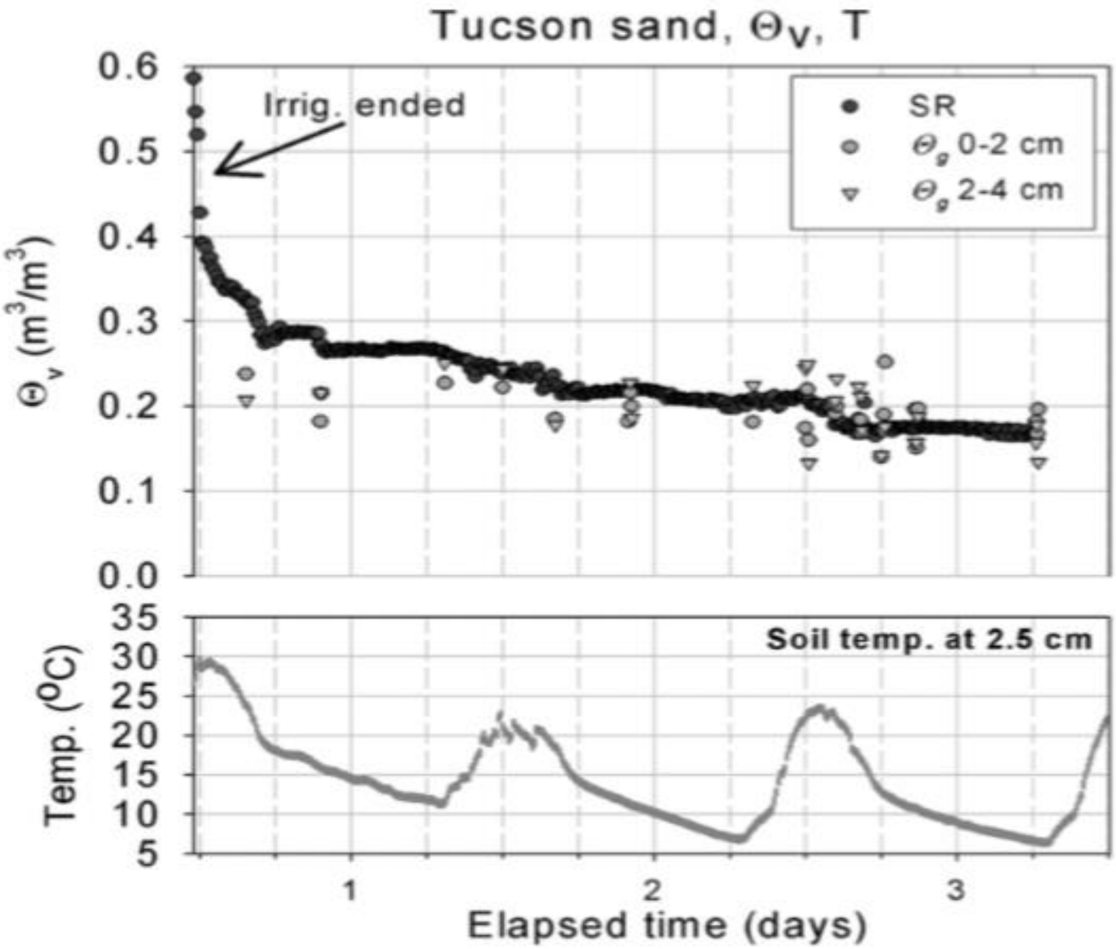

Figure 2: GPR measurement of soil water content over Tucson sand in November 2001, with gravimetric WC data and variation in top 2.5 cm temperature. Time is elapsed from 0:00 on November 12, 2001. (Or, and Serbin, 2004) [10]

In a study by Igel et al. (2011) [13] to identify the influence of the soil on the performance of GPR for landmine detection, the researchers use electric resistivity tomography (ERT), time domain reflectometry (TDR), and GPR in order to measure the electric and dielectric properties of different soil. They found out that the permittivity fluctuations caused larger influence on the performance of GPR compared to conductivity fluctuations. The study uses both geostatic and geophysical methods in order to classify the soil according to the ability of GPR to detect landmines. Results show the impact of soil properties on the performance of the GPR. Table 3 provides a summary of their findings.

Table 3: Qualitative evaluation of measured soil properties and estimation of soil impact on the performance of GPR. λ: dominant wavelength. (Igel et al., 2011) [13]

phys. property	"Sand"	"Laterite"	"Humus"
absolute level of σ	very low	low	low
spatial variability of σ	very small	large	large
spatial pattern of σ	$> \lambda$	$> \lambda$	$\approx \lambda$
attenuation	very low	low	medium
absolute level of ε_r	low	high	high
spatial variability of ε_r)	very low	large	very large
spatial pattern of ε_r	$\gg \lambda$	$> \lambda$	$\approx \lambda$
predicted soil influence	very low	medium	strong

Osman and Siddiqui (2012) [14] conducted research in order to assess the ability of nondestructive methods to determine soil's properties. The purpose of their study is to determine the capability of a cheaper method to study soil's properties instead of the time consuming and expensive approach of digging boreholes. The researchers also study the ability of the electrical resistivity method in correlating properties, such as moisture content, cohesion, angle of internal friction, and unit weight. Results show a strong correlation between electrical resistivity of the soil and water content and angle of friction. However, results do not indicate a strong relation between the electrical resistivity and cohesion and unit weight of the soil. The results showing the correlations found in the study is illustrated in Figure 3.

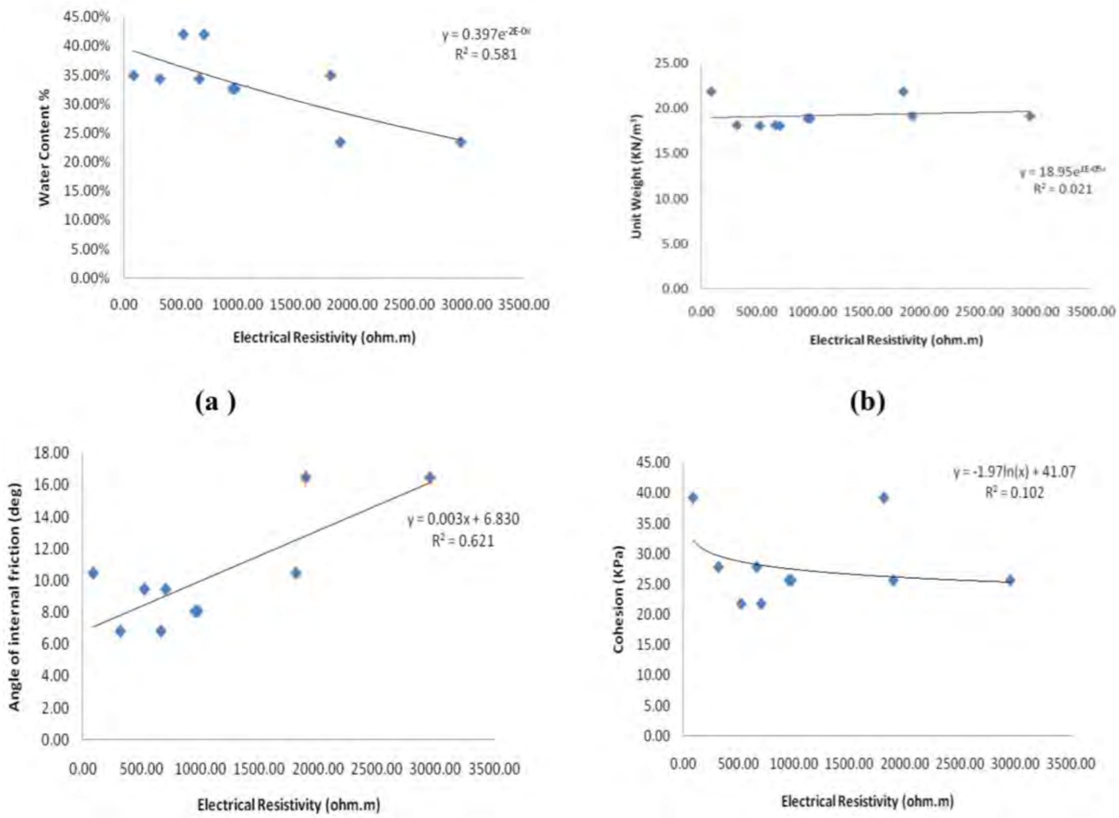

Figure 3: Correlations of electrical resistivity with (a) moisture content (b) unit weight (c) Angle of internal friction, and (d) Cohesion of soil. (Osman, and Siddiqui, 2012) [14]

Abidin et al. (2013) [15] conducted a research study using electric resistivity method (ERM). The purpose of their study is to demonstrate the effect of soil's water content and grain size distribution on the electrical resistivity of the soil. Thus, they measured the soil's resistivity for different samples of soils with different gradation and water content. Results show that the electrical resistivity decreased as the grain size of the soil increased. Similarly, the electrical resistivity of the soil also decreased with the increase in the soil's water content. The result of Abidin et al. (2013) [15] study is demonstrated in Figure 4.

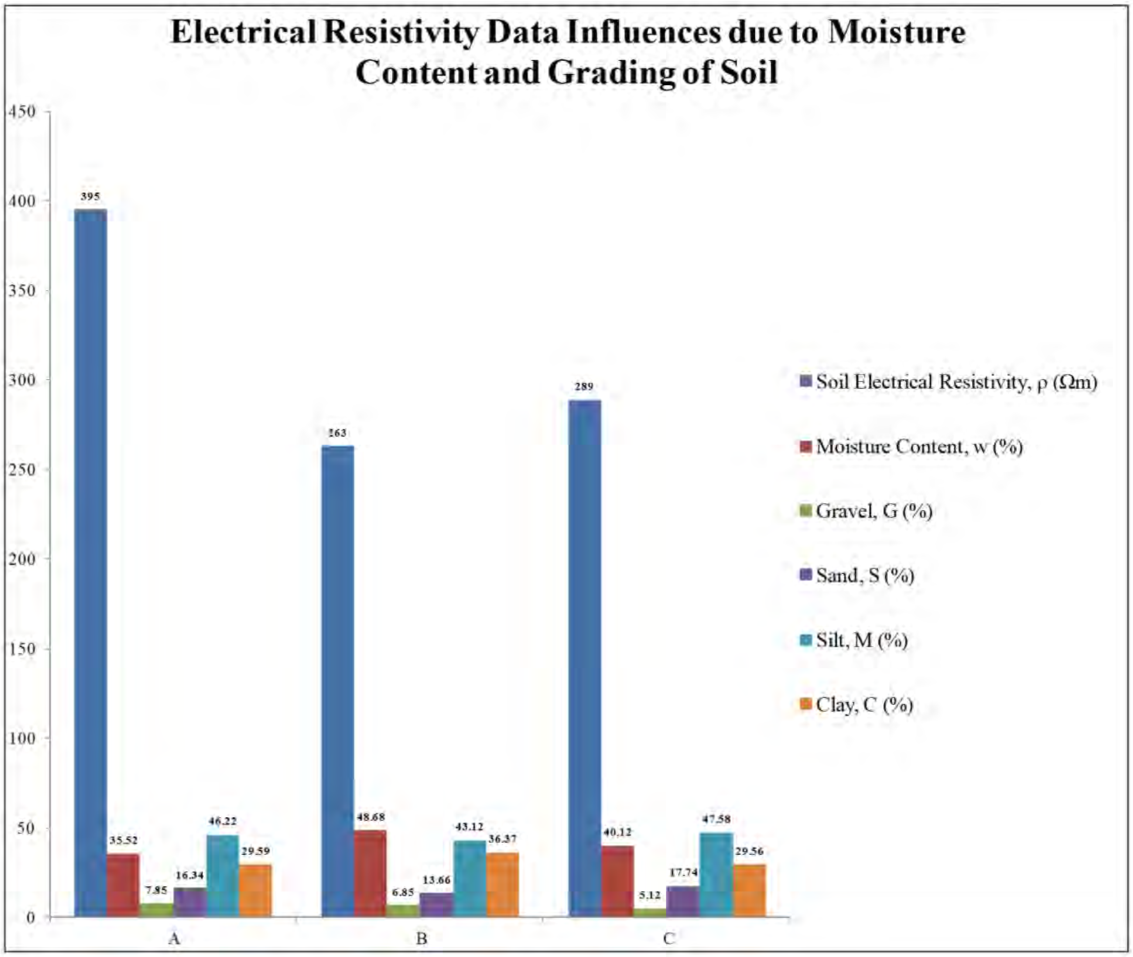

Figure 4: Overall results from field resistivity test and geotechnical lab test from point A, B, and C. (Abidin et al., 2013) [15]

Fallah-Safari et al. (2013) [16] carried out a study in order to study some clay's properties by using nondestructive technique. The purpose of the study is to provide alternative nondestructive technique as an alternative to the expensive geotechnical tests. The researchers use the electrical resistivity method in order to determine the relation between the water content, void ratio, and density of the clay. Results show that the electrical resistivity decreased as the water content of the clay increased. Moreover, as the void ratio increased, the electrical resistivity of the clay increased. The relation found between the water content and electrical resistivity of the clay is demonstrated in Figure 5.

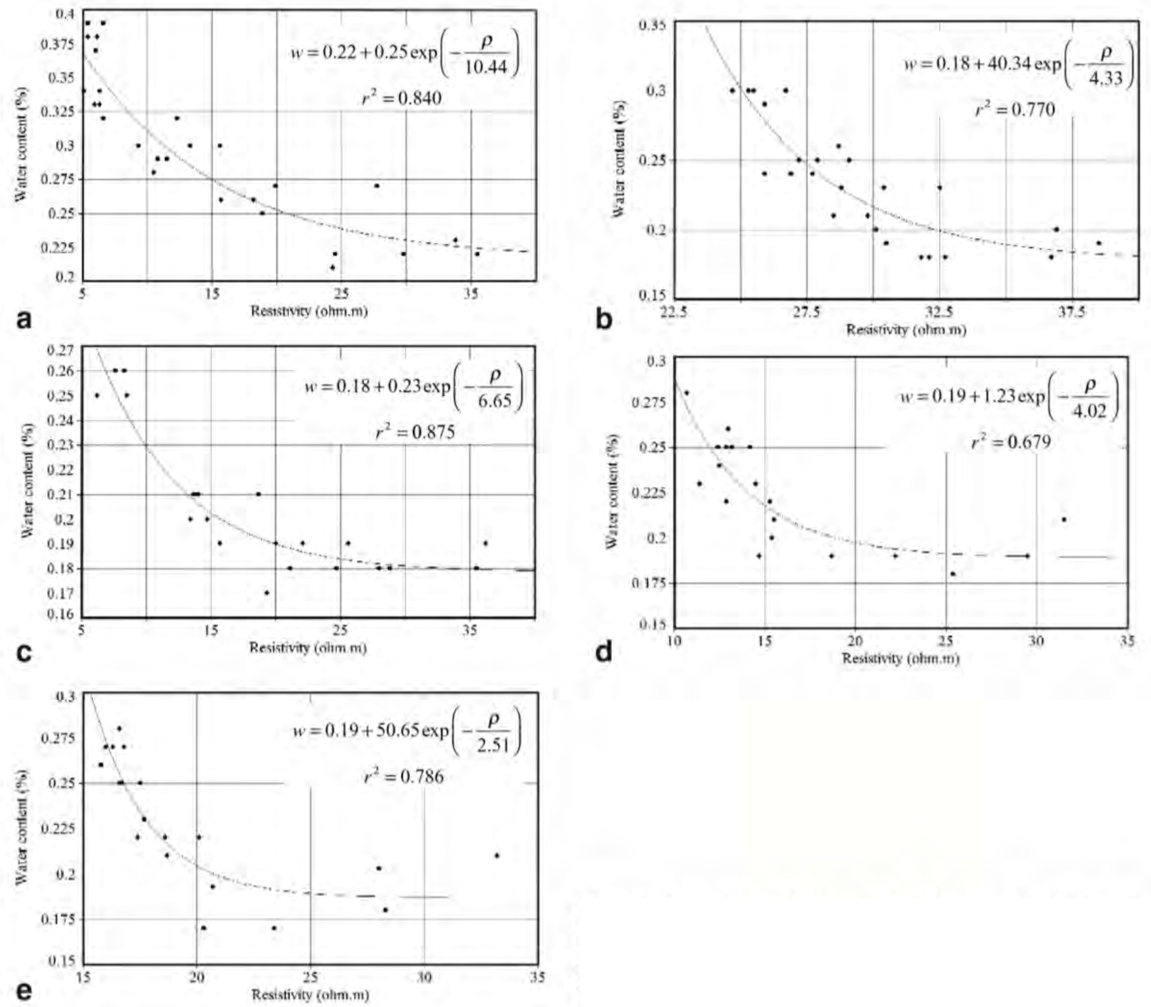

Figure 5: Relationship between clay electrical resistivity and water content: a) bentonite; b) kaolinite; c), d) and e) are three samples that were collected in different places around Karaj, Iran. (Fallah-Safari et al., 2013) [16]

2.3 GPR for Measuring Water Content

Allison et al. (1988) [17] carried out a research study to assess the suitability of ground penetrating radar in determining the lateral extent and depth of diagnostic subsurface features and their spatial variability. Their study shows that the GPR was able to detect the depth to argillic horizons and their spatial variability. Moreover, the study uses the GPR to detect the contact depth to geologic materials that underlie sand deposits. Results indicate that GPR could be used to monitor the subsurface features that have contrasts in their dielectric constants. The researchers illustrate the ability of GPR to determine the depth in comparison to the measured depth in Figure 6.

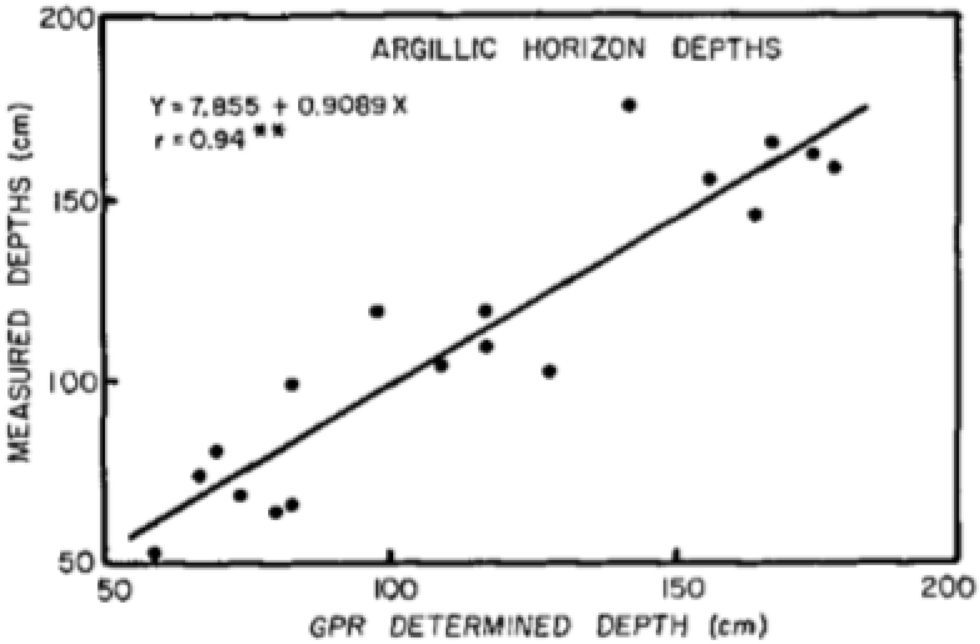

Figure 6: Relationship between physically measured depth versus depth determined by ground penetrating radar. (Allison et al., 1988) [17]

Collins and Doolittle (1995) [18] assess the suitability of using ground penetrating radar in order to determine soil characteristics. They indicate that the main challenge when using GPR is the high conductivity of a soil sample. However, this problem can be solved by using an antenna with low frequency. Nonetheless, this will also reduce the imaging resolution. The researchers [2] point out that several factors influence the soil conductivity; for instance, water content, degree of saturation, porosity, the amount and type of the salt present in the sample, and the amount of clay. However, the GPR was found suitable for collecting data in the shallow depths (i.e., depths <30m) in comparison to other nondestructive methods. Results of GPR tests on soil with different moisture contents as tested by Collins and Doolittle (1995) [18] are shown in Figure 7.

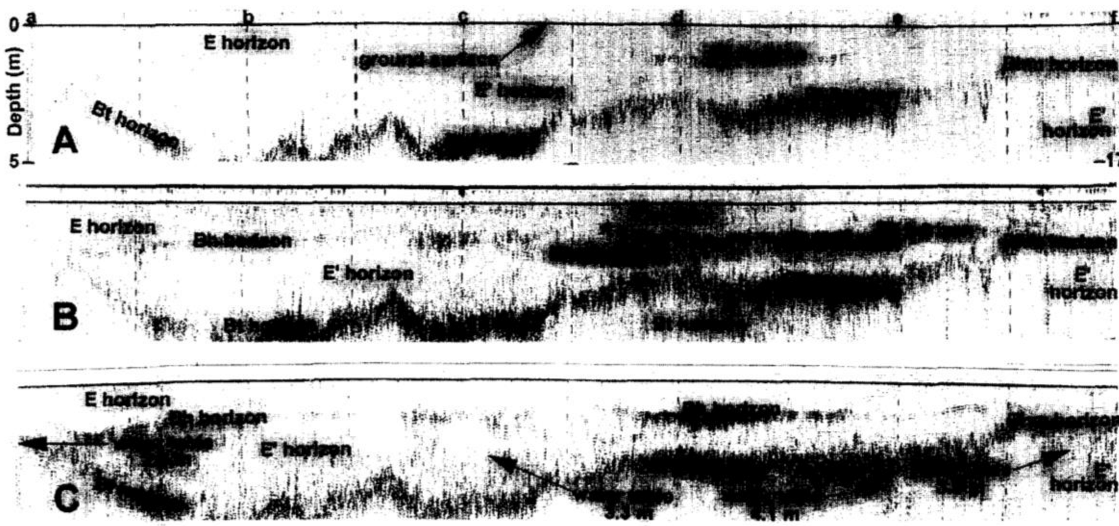

Figure 7: (a) Soil radar profile during a dry soil moisture period, (b) Soil radar profile during a moist soil moisture period, and (c) Soil radar profile during a saturated soil moisture period. (Collins, & Doolittle, 1995) [18]

Gehrels et al. (1997) [19] assess the capability of ground penetrating radar to measure the water content of unsaturated sandy soil in Netherlands. Using the GPR is advantageous in estimating that water content of the soil using nondestructive method without a need for soil drilling. In order to verify their results, the researchers compare the data measured by the GPR with the data collected from accessing tubes using capacitance probe. They point out that the water content measured with GPR was accurate, and this is due to the contrasting dielectric constant of the soil. They demonstrate the agreement in soil water content measured from two sites using GPR versus that measured by capacitance probe in Figure 8.

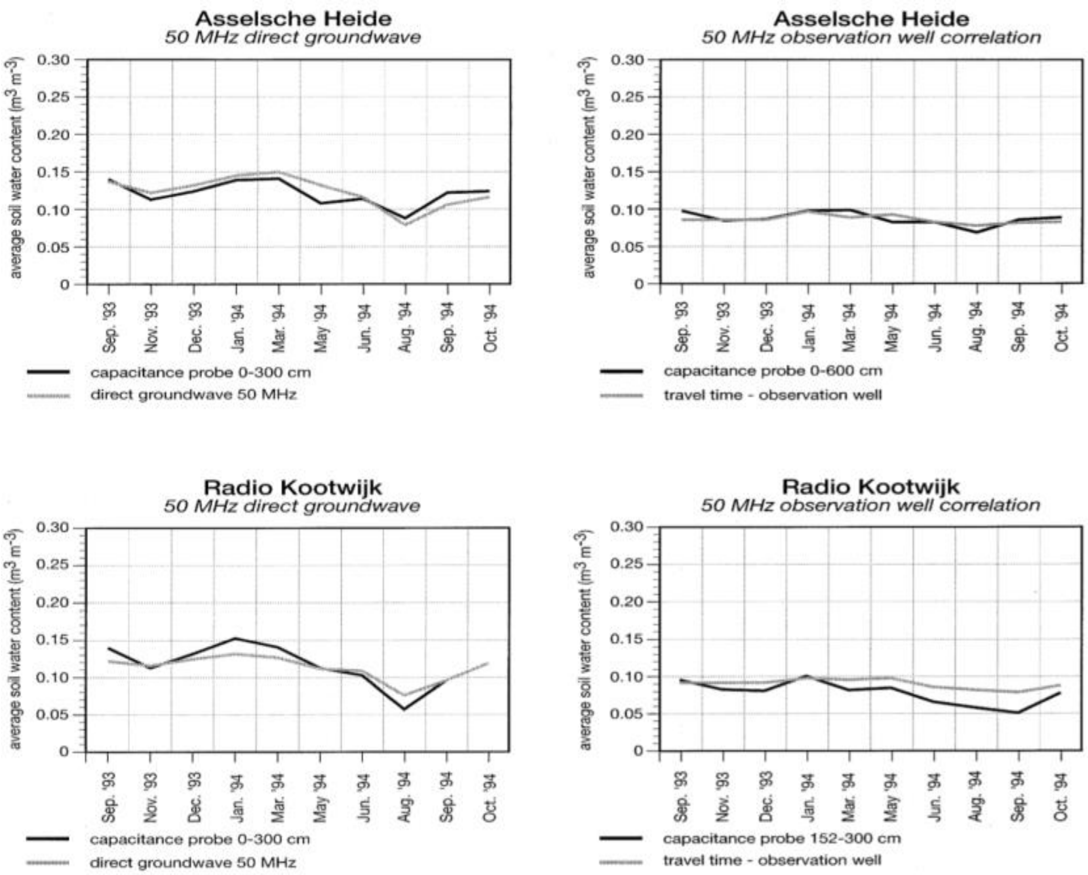

Figure 8: Soil water content variations deduced from direct 50 MHz radar waves and from correlations between the ground water reflector (50 MHz) and well observations, compared with capacitance probe measurements at AsselscheHeide and Radio Kootwijk. (Gehrels et al., 1997) [19]

Hubbard et al. (2005) [20] carried out a study in order to assess the ability of the ground penetrating radar in measuring soil water content at different degrees of soil saturations. They use the GPR reflections travel time in addition to the depth of the reflector in order to calculate the dielectric constant for the soil above the reflector. Moreover, the study uses site relationship between the volumetric water content (VMC) and the dielectric contestant in order to estimate the VMC for the soil above the reflector. Figure 9 illustrates using the site relationship with the VMC.

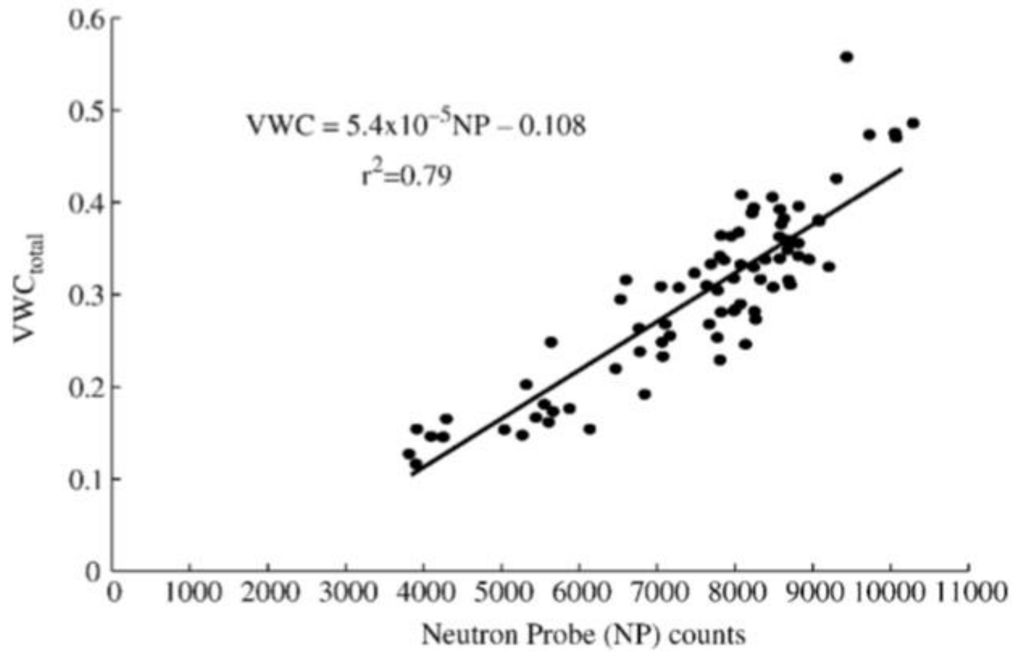

Figure 9: Site-specific calibration between neutron probe (NP) counts and total volumetric water content (VWC). Data was collected under both dry and wet conditions. (Hubbard et al., 2005) [20]

Lambot et al. (2006) [2] propose an inverse modeling approach of nondestructive procedure in order to determine near-surface hydraulic properties and electric profile by using GPR data. They indicate that air entry value parameter (α) and pore size distribution parameter (n) are negatively correlated. However, they point out that the saturated hydraulic conductivity (k_s) was positively correlated to saturated water content (Θ_s) and to tortuosity (λ).

Turesson (2006) [1] demonstrates the ability of nondestructive methods, such as GPR and the resistivity method, in finding the water content of a soil sample that consists of sand and gravel. A representative soil sample was collected at a depth of 1 m. The main challenge in this study was that, in order for the GPR to be able to measure the water content, the sample must have variations in the dielectric constant. Furthermore, according to Turesson (2006) [1], the GPR method is limited in case of conductive materials, like clayey soil or soil, that is saline. However, the researcher was able to measure the water content of the soil sample by using the GPR, and the resistivity method. The results of both methods show similar trends. Figure 10 shows an example from Turesson's [1] work of common midpoint method (CMP) measurements used in the velocity analyses with a one-dimensional velocity model, hyperbolic adaptions and semblance images at 30 m. Moreover, Figure 11 was deduced by Turesson [1] in order to show the GPR's two-dimensional interval-velocity profile constructed from 21 one-dimensional velocity models.

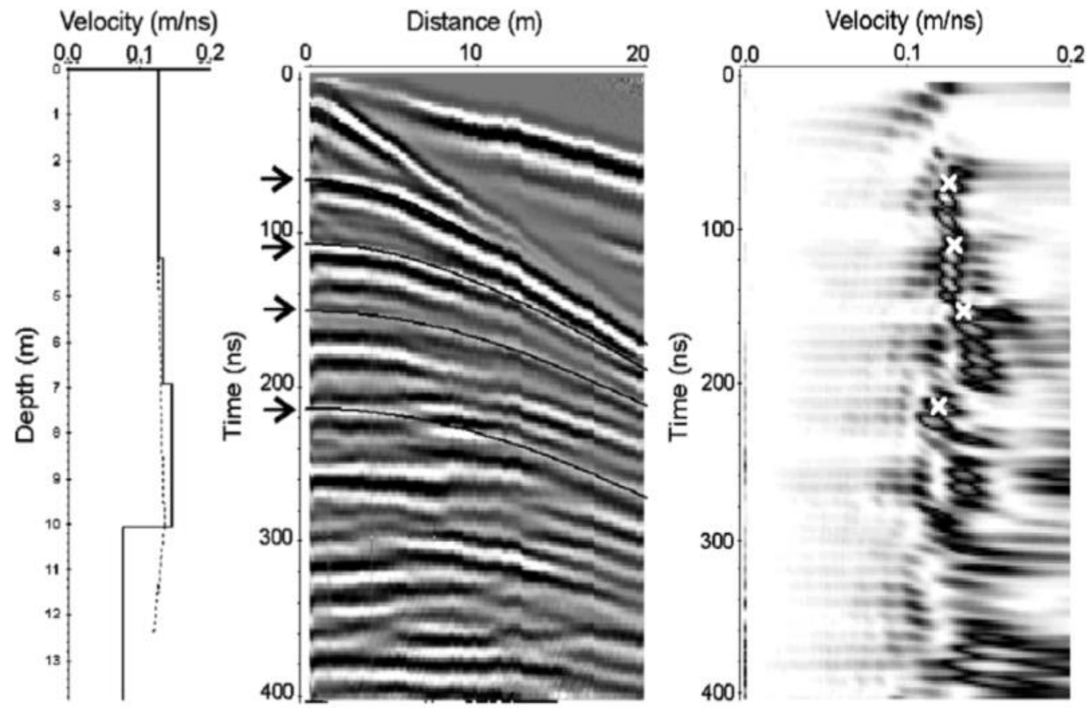

Figure 10: Example of CMP measurements used in the velocity analyses with a one-dimensional velocity model, hyperbolic adaptions, and semblance images at 30 m. (Turesson, 2006) [1]

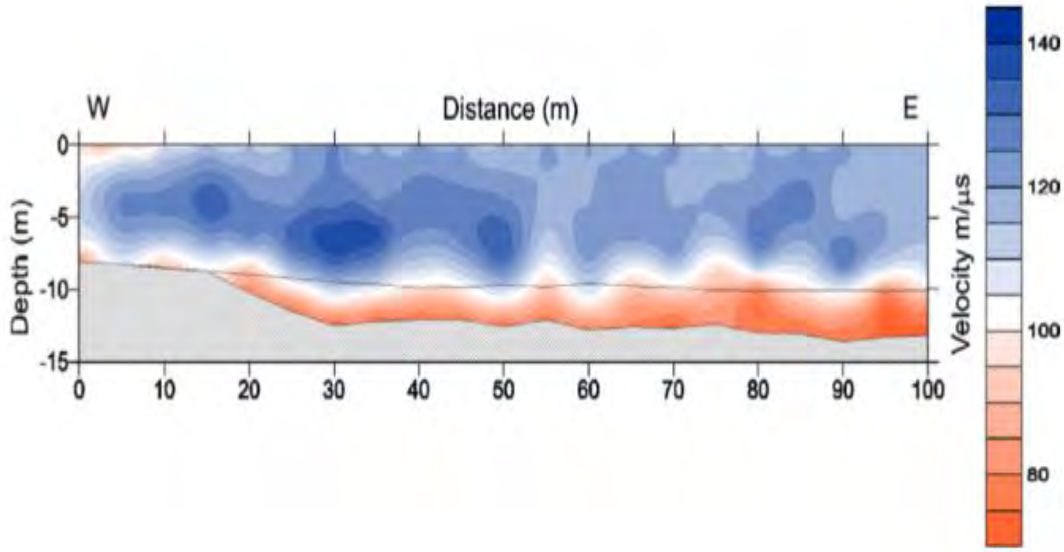

Figure 11: The GPR two-dimensional interval-velocity profile constructed from 21 one-dimensional velocity models. The continuous line shows the water table deduced from seismic refraction. (Turesson, 2006) [1]

Cui et al. (2012) [21] carried out a research study in order to develop a new electrical resistivity probe to be able to monitor the change in water content of the soil nondestructively. All nondestructive methods work by measuring the soil's resistivity and relate it to other parameters like water content. The goal of the study is to establish a relationship between changes in soil's resistivity and changes in water content. Thus, the study measures the resistivity for six soil samples with different water contents. The electrical resistivity versus soil's water content and degree of saturation is shown in Figures 12 a and b.

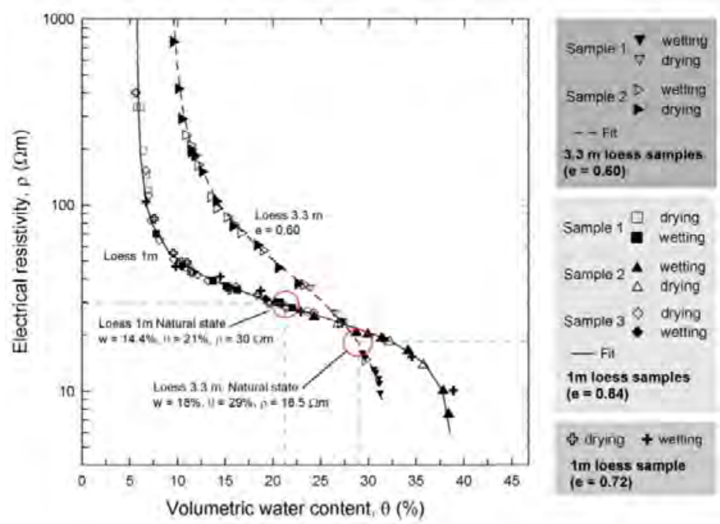

(a)

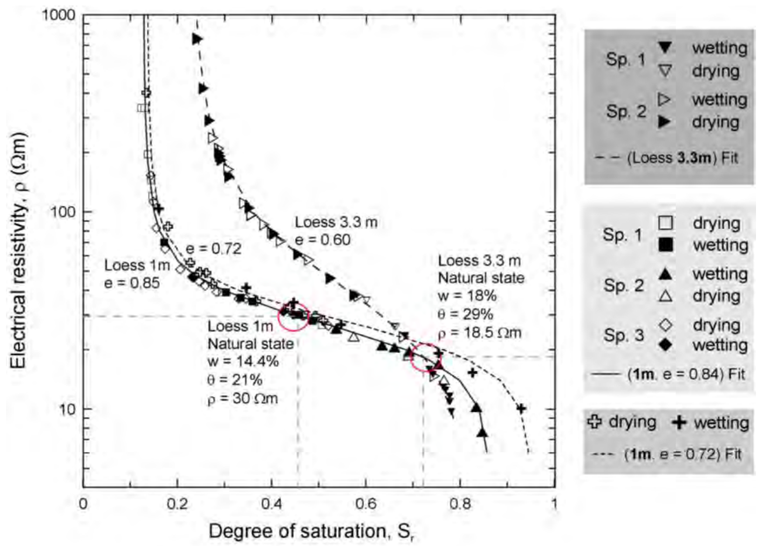

(b)

Figure 12: Resistivity data for loess at 1 m depth (e = 0.84 and e = 0.72) and 3.3 m depth. Electric resistivity versus (a) volumetric water content, and (b) degree of saturation. (Cui et al., 2012) [21]

Anbazhagan et al. (2013) [22] performed a study that used GPR in order to determine the homogeneity and compaction of the soil below a new constructed flooring slab. They use a wave form character in their study in order to assess the compaction of the soil. Thus, a strong GPR wave reflection was noticed for less saturated and high density. On the other hand, distorted waves were noticed for loose and saturated section. In addition, the researchers indicate that if the wave character is changing, this means that there is heterogeneity in the compaction. In addition, they point out that when the wave amplitude changes for a particular layer, this means a decrease in water content which indicates a loose compaction.

Another study that was conducted by Anbazhagan et al. (2013) [23] uses ground penetrating radar to investigate the degree of compaction of soil fill. The researchers constructed various controlled model sections in the laboratory in order to determine the results obtained by GPR in different compactions of soil and different degrees of saturation. They indicate that the wave amplitude decreased when the moisture content of the soil increased. The researchers conclude that interpretations from GPR radargram can be used in order to investigate soil different degrees of compaction. They show homogeneous and heterogeneous soil layers deduced from GPR radargram in Figure 13.

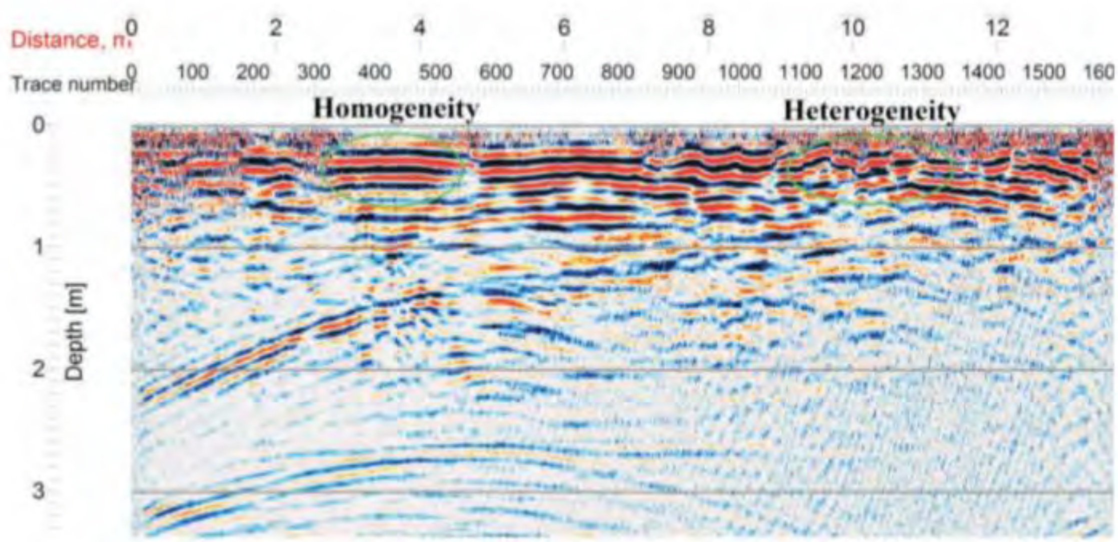

Figure 13: Typical radargram showing homogenous and heterogeneous soil layer. (Anbazhagan, et. al. 2013) [23]

2.4 Summary of the Literature Review

Based on the discussion above, the only soil property that was measured by several researchers is the soil water content, and soil homogeneity. Soil homogeneity was used indirectly as a reflection of soil compaction. Nonetheless, other significant soil properties; for example, soil's void ratio, gradation, and friction angle, have not been considered in depth in any research work. Internal friction angle is a major shear strength parameter of soil, especially sandy soil. It is used together with soil unit weight to estimate the soil bearing capacity for shallow foundation, and pile capacity in deep foundation. Moreover, void ratio is another important parameter of the soil. It must be taken into consideration during the design process since it can be related to settlements of structures. Thus, an important goal of this research is to relate the friction angle to void ratio and grading of the soil and then relate all major soil properties to soil resistivity or conductivity.

Chapter 3: Methodology

3.1 Experimental Setup

This research aims to predicate several soil properties utilizing data from the nondestructive equipment (GPR) to be used in the study. To achieve this goal, the experimental investigation is divided into two categories. The first one is the index test category, which is conducted to measure the soil resistivity on small compacted samples of different soils. In this category, four soil samples with different gradations passing sieves, no.4, no.8, no.16 and no.50, are tested. The second test category is the application tests, which is conducted to test the applicability of the GPR on a field soil profile. In this category, two different soil samples with different gradations are used. The original Ras al-Khaimah (RAK) soil passing and modified RAK soil (passing sieve no.8) are used. Procedures followed to collect data from both categories are discussed in the following sections. Figure 14 summarizes the steps that are followed in this research.

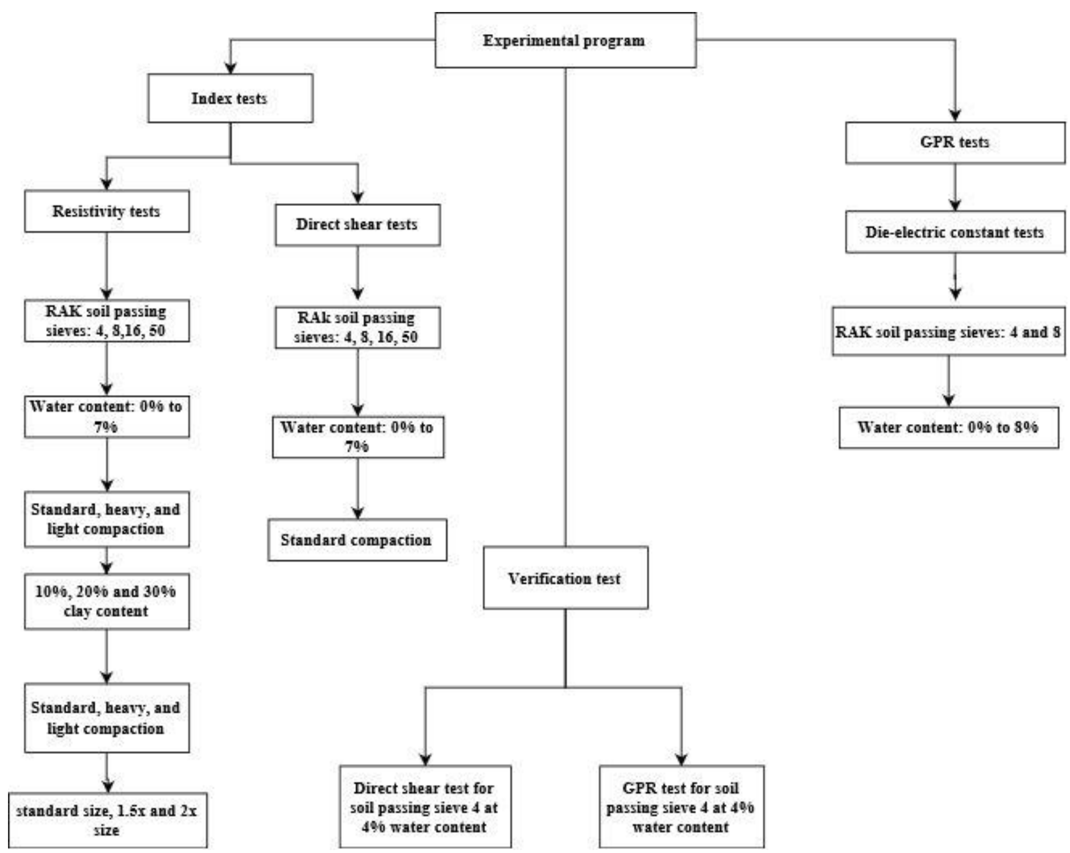

Figure 14: Summary of research methodology

3.2 Category I: Index Tests

3.2.1 Effect of water content on soil's resistivity. The procedure followed to conduct this test is as follows:

- A sieve analysis is done to determine gradations for the four different soil used in the study.
- The change in resistivity with the change of the water content is measured for each of the three soils used.

The schematics and apparatus used in the experiment are shown in Figure 15.

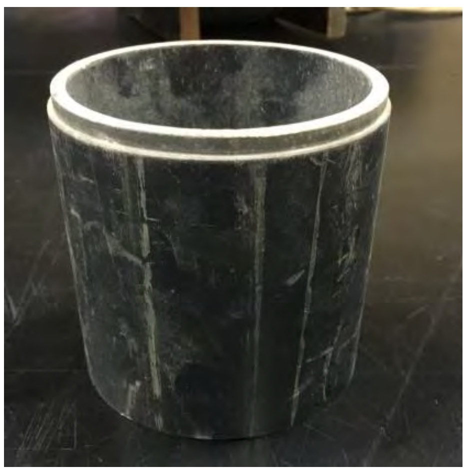

a: Standard mold

b: Digital balance

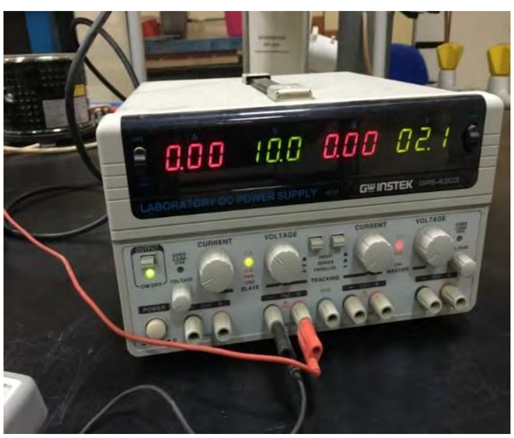

c: Voltage (V_s) source

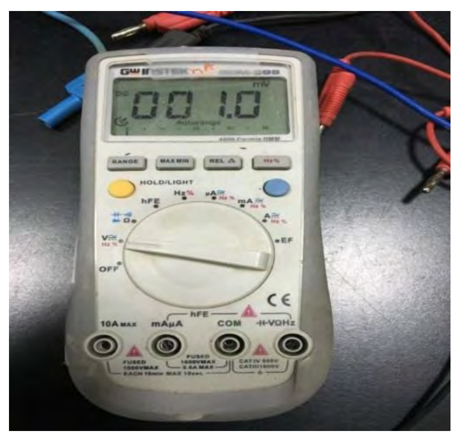

d: Voltmeter and Ammeter

e: Source of known resistance (R_1)

Figure 15: Devices used to find the resistivity of the soil with varying water content

A standard compaction test is done by using a standard mold with known Height (H), Length (L) and Diameter (D). The following steps are followed for each soil sample:

1. The soil is first mixed with an initial water content of 7%.
2. Then, the mold is filled into three layers and compacted by hammering 25 blows as a standard compaction test.
3. A metallic sheet is placed below and another one above the soil sample.
4. The balance is then used to measure the weight of the sample.
5. After that, the soil sample is connected to a source of voltage (V_S) and another resistor (R_1) with known resistance in ohms (Ω).
6. Next, a known voltage (V_S), in volts, is applied through the circuit. A voltmeter could be connected to the circuit to measure the voltage passing across the soil sample (V_{RS}) and through the known resistor (V_{R1}).
7. An ammeter is then connected to the circuit to measure the current (I), in milliamperes (mA), passing through the circuit.
8. After that, check that $V_{RS} + V_{R1} = V_S$ is satisfied; otherwise, the work has to revised.
9. Similarly, check that $R_1 \times I = V_{R1}$ is satisfied; otherwise, the work has to be revised.
10. After that, the resistance of the soil sample (R_S) is calculated in ohms (Ω), using Eq 2:

$$R_S = \frac{V_S}{I} - R_1 \text{ .... Eq 2.}$$

11. In addition, the resistivity ρ of the soil sample is calculated in ohms.cm (Ω.cm) using Eq 3:

$$\rho = \frac{R_S A}{L} \text{.................................. Eq 3.}$$

12. The soil sample is then removed of the mold and placed in the oven for two hours to dry.
13. The weight of the soil sample and its resistivity are measured by following steps 2-11 above. This reading represents the resistivity of the soil with that water content before waiting for 24 hours (immediately after drying) for the water to be in equilibrium.
14. Next, the soil sample is wrapped in a plastic bag and left for 24 hours, so that the water will be in equilibrium. Then, the weight of the soil sample and its resistivity are measured. This represents the resistivity of the soil with that water content after waiting for 24 hours for the water to be in equilibrium.
15. Finally, this procedure is repeated until the water content of the sample reaches 0.

In order to find the resistivity of the soil sample for different compaction efforts, the above steps are followed. However, the mold was compacted by 10 blows instead of 25 blows. Moreover, the same steps are followed for heavy compaction but instead the mold is filled into five layers, and 25 blows are applied for the compaction.

3.2.2 Effect of mold size on soil's resistivity. This test is done using heavy compaction for the soil passing sieve no.16. In this test a standard mold, one and a half times a standard mold, and two times a standard mold sizes are used. These three molds are shown in Figure 16.

Figure 16: Standard mold, 1.5 x standard mold, and 2 x standard mold

The steps followed for this test are the same as those followed in section 3.2.1. However, for the 1.5 x standard mold, the mold is filled into 7 layers, and a compaction of 25 blows is used. On the other hand, the 2 x standard mold is filled into 10 layers, and 25 blows are used for compaction.

3.2.3 Effect of particle size on soil's resistivity. This test is done on soils with different particle sizes; for instance, the soil used in section 3.2.1, and different compaction efforts. However, tests are conducted on the samples after 24 hours of drying. This leads to more consistent and more realistic observations.

3.2.4 Effect of void ratio on soil's resistivity. This is done by calculating the void ratio (e) from the data collected earlier for the three different soil samples with different compaction efforts. Test data for experiments conducted after waiting for 24 hours for the water to be in equilibrium is used in the calculations. Moreover, the void ratio is calculated by using Eq 4:

$$e = \frac{V_V}{V_S} \qquad \text{Eq 4.}$$

Where V_V represents the volume of the voids, and V_s represents the volume of the solid. Moreover, V_v and V_s are calculated since the water content, weight of wet soil, weight of water and the specific gravity G_s of the soil (2.65) are known.

3.2.5 Effect of 24 hour time lag on soil's resistivity. This comparison is made by comparing the different resistivity values for the different soil samples passing sieve no.16. The values collected from section 3.2.1 to compare the difference of waiting 24 hours on the resistivity of the soil with different water contents for different compaction efforts are used in the comparison.

3.2.6 Effect of clay content on soil's resistivity. This test uses the soil sample passing sieve no.16 mixed with 10%, 20%, and 30% of clay. The standard compaction procedure is followed to measure the resistivity of samples with different water and clay content. The resistivity of the sample is measured by following the steps in section 3.2.1. However, this is done after waiting for 24 hours, so that the water is in equilibrium after drying the sample each time.

3.2.7 Effect of water content on soil's friction angle. In this test, four different gradations of soil are used to investigate the effect of varying water content on the friction angle of the soil. For each sample of soil, the friction angle is measured at 0%, 4%, and 8% water content. The friction angle is calculated after performing the direct shear test, as shown in Figure 17, by following these steps:

1. The soil sample is first prepared in its mold.
2. The consolidation stage of the direct shear test is performed by using a normal stress (σ) caused by applying a 1Kg load.
3. The researcher waits until there is no more displacement in the vertical direction in order to start the shearing stage of the test.
4. The shearing stage is then started, and the researcher waits until a shearing failure occurs.
5. The peak shear strength (τ) applied is written down to be Plotted later on.
6. Steps 3-5 are repeated using 2Kg and 4Kg loads, respectively.
7. Microsoft Excel is used to draw the graph of normal stress versus the peak shear strength and find an equation of the best fit line.
8. The friction angle (Φ) is then found by calculating the $\tan^{-1}$ of the slope of the line.

9. Finally, steps 1-8 are repeated for the four types of soil at 0%, 4%, and 8% water content.

Figure 17: Performing the direct shear test

3.3 Category 2: Application Tests

3.3.1 Effect of water content and compaction effort on dielectric constant of soil 1. In this section, the original RAK soil is used to determine the effect of varying the water content (0%, 2%, 4%, 6%, and 8% water content) and the compaction effort on the dielectric constant of the soil. In order to determine that, the GPR is used, and a steel plate is placed at a known depth inside a wooden box that has the dimensions of 1.5 m x 0.9 m x 0.5 m. The following steps are followed in this test:

1. A steel plate is placed at a known depth of 0.4 m in the wooden box as shown in Figures 18 a and b.

2. Half of the box (0.2 m) is filled with the dry soil and compacted using a compactor as shown in Figure 18 c.
3. The other half of the box (0.2 m) is filled with soil and compacted again using the same compaction effort as shown in Figure 18 d.
4. The box is then covered with a thin wooden sheet, and the GPR is used to determine the dielectric constant of the soil by trial and error. The objective is to determine the die-electric constant that show the known location of the steel plate (0.4m), as shown in Figure 18 e.
5. The soil is then removed from the box.
6. Around 2% of water (22 liters) is added to the soil as shown in Figure 18 f.
7. The soil is then mixed with the water until homogeneous is observed by the naked eye. After that, half of the box is filled with the wet soil, and compacted using the compactor.
8. The other half of the box is filled with soil and compacted again using the same compaction effort.
9. The box is then covered with a thin wooden sheet, and the GPR is used to determine the dielectric constant of the soil containing the selected water content.
10. A sample is taken from that soil and is dried in an oven to determine the percentage of its moisture content.
11. Another 22 liters of water are added to the soil, and steps 7-10 are then repeated. This step is repeated twice.
12. Next, another 15 liters of water are added to the soil and mixed until homogeneous mix is achieved. This is determined by observation.
13. The whole box is filled with the soil without compaction, and the die-electric constant of the loose soil is measured using the GPR without compaction.
14. Then, half of the soil is removed from the box, and the other half remaining in the box is compacted.
15. The other half of the box is then filled with the same soil and compacted. After that, its dielectric constant after compaction is measured.
16. A sample is taken from that soil and is dried in an oven to determine the moisture content.

17. Finally, the RADAN software is used to process the images collected by the GPR in order to remove background effects.

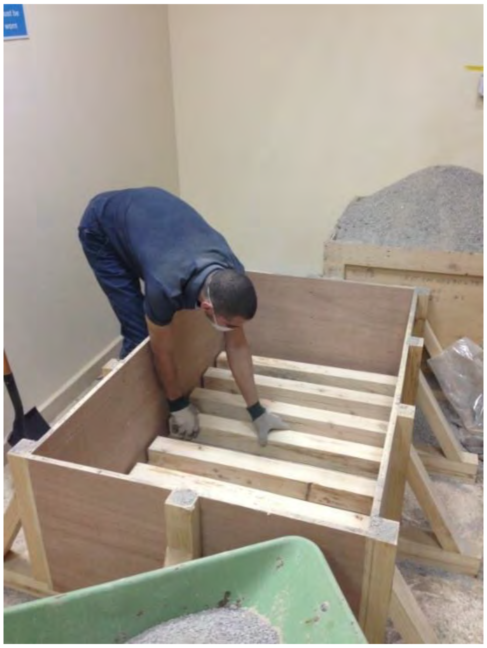

a: Wood supports

b: Steel plate placed at a depth of 0.4 m in the box.

c: Compaction 1st layer (0.2m)

d: Compaction 2nd layer (0.2m) of the box

e: Using the GPR to find the die-electric constant. f: Mixing the water with the soil.

Figure 18: Steps to determine die-electric constant of a soil

3.3.2 Effect of water content and compaction effort on dielectric constant of soil 2. In this section, the modified RAK soil (passing sieve no.8) is used to determine the effect of varying the moisture content (0%, 2%, 4%, 6% and 8% water content of the soil weight) and the compaction effort on the dielectric constant of the soil. To determine that, the same procedure discussed in section 3.3.1 is followed.

Chapter 4: Results and Discussion

4.1 General

This chapter is divided into two main sections: index tests, and large scale application tests. Index tests include resistivity and direct shear tests for different soil parameters; whereas, the GPR is used for the large scale application tests to determine dielectric constant for different soil properties. Results of the small index tests are reported and discussed first and then followed by a presentation and discussion of the results of the large application tests. In the second section of the chapter, both results are correlated in order to connect both soil resistivity and dielectric constant to different soil properties.

4.2 Materials

As mentioned earlier in chapter 3, three different soils with different gradations are used in this study. However, all soils are extracted from the RAK original soil by sieving them at different sieve sizes. Soil passing sieve No. 4 is the original RAK soil but slightly modified by sieving on No. 4 sieve to remove the small portion of gravel that might be included. Similar modification has been conducted for soils passing No. 16 and No. 50 in order to obtain more fine graded soils. Grading curves for the three soils are shown in Figure 19. It could be noticed that soil passing No. 50 is finer than soil Passing No. 16, and both are finer than the modified RAK soil which is passing No. 4 sieve. All soil samples have been classified according to the Unified Soil Classification System (USCS) (ASTM 2000), and results of classifications and other gradation properties are shown in Table 4.

Table 4: Different soil gradation parameters and soil classification

Soil Type	$C_u = D_{60}/D_{10}$	$Cc = (D_{30})^2/(D_{10}\ D_{60})$	Soil Classification
Soil passing No. 4	5.09	1.88	SW
Soil passing No. 8	5.00	1.03	SW
Soil passing No. 16	3.06	0.58	SP
Soil passing No. 50	2.44	1.20	SP

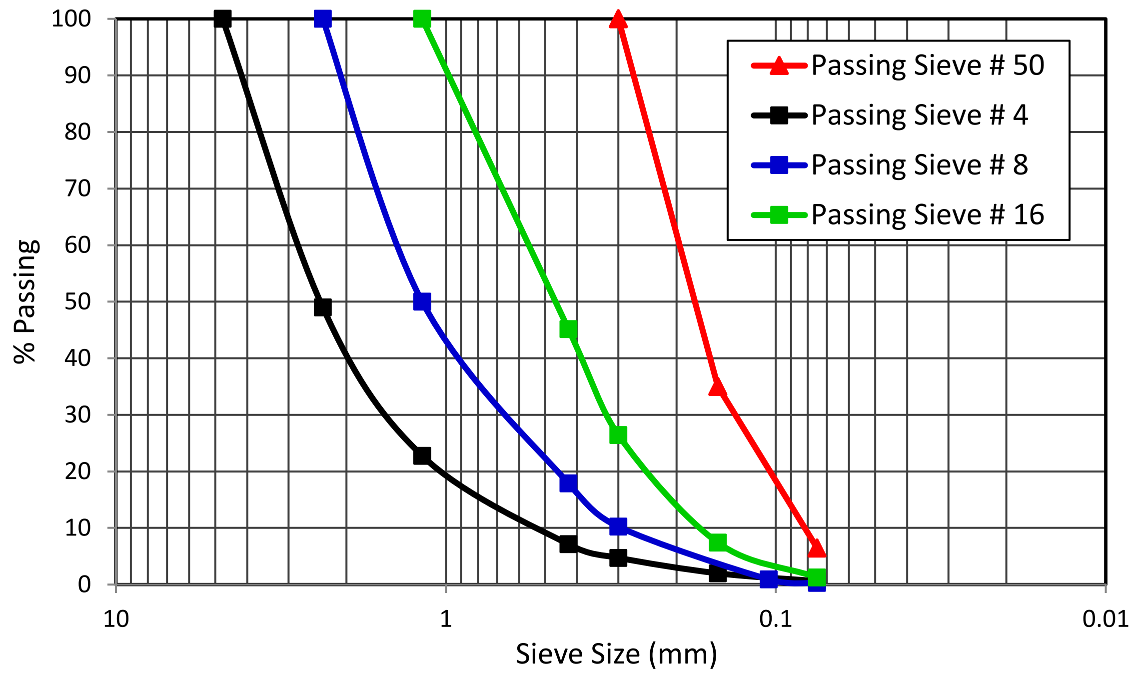

Figure 19: Grading curves for the four different soils used in the current study

4.3 Results of Index Tests

In order to select the index tests mold size, different sizes have been tried, all of them with the same diameter which is about four inches to match the standard proctor mold. In this task, three mold heights are selected: standard height, 1.5 times the standard height, and 2 times the standard height. Compaction effort for each size has been calibrated based on the energy equation suggested by Das and Sobhan (2014) [24] (i.e. Equation 5). This equation is used to calculate the compaction energy (E) based on the number of soil layers, number of blows per layer, weight of hammer, height of the hammer drop, and volume of the mold. This calibration ensures that the compaction effort is similar for all sizes, and the mold size is the only parameter that is in charge in this case. Soil passing No. 16 sieve is selected to be used in these tests. Resistivity readings are taken 24 hours after soil specimens are taken out of the oven. Results of this sensitivity analysis are shown in Figure 20 which clearly shows that the mold size has an insignificant effect on the soil measured resistivity for the same compaction energy. This result is true for all water content percent used in this analysis. Therefore, the standard mold size is used in all index tests that follow. More results are in Tables 5 and 6 in Appendix A.

$$E = \frac{\begin{bmatrix} Number\ of \\ blows/layer \end{bmatrix} x \begin{bmatrix} Number\ of \\ layers \end{bmatrix} x \begin{bmatrix} Weight\ of \\ hammer \end{bmatrix} x \begin{bmatrix} Drop\ height \\ of\ hammer \end{bmatrix}}{Volume\ of\ mold} \quad \text{..................Eq 5.}$$

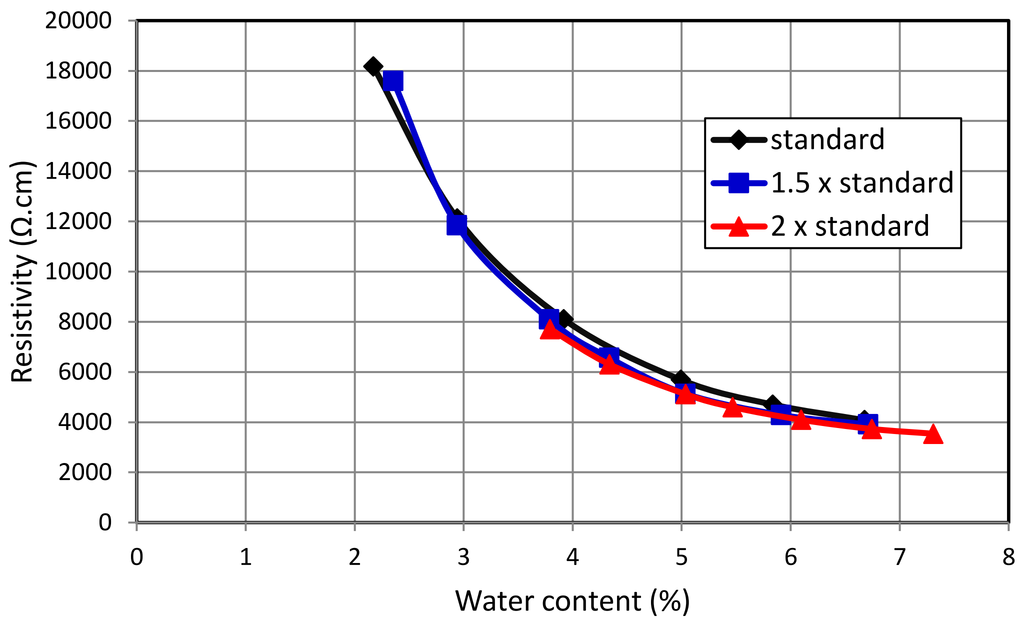

Figure 20: Effect of mold size on soil resistivity for soil passing No. 16 sieve

4.3.1 Effect of Water Content on Soil Resistivity. The index tests have been conducted in order to study the effect of different soil parameters, such as water content, void ratio, gradation, degree of saturation, and clay content on the soil resistivity. In order to measure the effect of water content, and degree of saturation on resistivity of soil, different samples have been compacted at their optimum moisture content and dried gradually, both in the oven and in the air. This process reduces the water content and degree of saturation, and it maintains other properties of soil as is, which allows one parameter to be isolated on time. For each specimen, resistivity is measured twice at approximately the same water content; one measurement was taken just after the specimen is taken out of the oven, and the other measurement was taken after leaving the specimen 24 hours in a plastic bag. Leaving the soil specimen in a plastic bag for 24 hours in the lab temperature is expected to equilibrate the water content percent throughout the specimen, and it might affect the measured resistivity. In other words, it is expected that the surfaces of the specimen, when removed from the oven, are drier than the sample inside. Moreover, storing the specimen inside a plastic bag for 24 hours allows the insider water to migrate towards the dry surfaces. This process leads to a water content equilibrium throughout the soil specimen.

Figures 21-23 show the variation of soil resistivity versus water content percent for soils passing No. 4, No. 16, and No. 50 sieves, respectively. The figures also illustrate the effect of compaction effort, and time after removing the specimen from the oven. Soil passing No. 4 is known to be the coarse grained sandy soil among the three soil samples used in this study, as shown in Figure 19. Soil resistivity generally decreases as the soil water content increases, which is true for all soil types tested in this research work. This conclusion is demonstrated in Figures 21-23 regardless of the compaction effort, soil type, and time left for water content equilibrium. This result is attributed to the small resistivity of the water compared to soil particles. Therefore, as the water content inside the soil pores increases, the resistivity of the soil/water mixture decreases. This also could be attributed to the increase in water continuity inside the pores, which is another factor of decreasing soil resistivity. Similar results were found by Cui et al. (2012) [21], Osman, and Siddiqui (2012) [14], and Abidin et al. (2013) [15].

With regards to the effect of compaction effort, Figures 21 and 23 indicate a significant effect of compaction effort on the soil resistivity versus water content. The effect of compaction effort is studied by compacting the soil specimens using standard proctor test, modified proctor test, and light compaction (10 blows/layer for three layers). For the same type of soil, as the compaction effort increases, the soil resistivity decreases at the same water content. This could be attributed to the reduction of the void ratio due to heavy compaction, and hence the more continuity of the water inside the pores. The more the continuity of water inside the soil pores is, the smaller the resistivity and the higher the conductivity. The opposite is true for the soil compacted lightly, where the voids have larger volume, and the water inside the voids suffers from discontinuity. Therefore, the lightly compacted soil shows small resistivity compared to the heavily compacted soil. Heavy compaction of a certain soil also decreases the void ratio and in turn increases the particles connectivity, which results in a reduction in the soil resistivity. Surprisingly, the soil with fine sand (i.e., soil passing No. 50 sieve) is highly affected by the compaction effort compared to soil with coarse sand (i.e., soil passing No. 4 sieve). For soil passing No. 16 sieve (i.e., the coarse to fine grained sandy soil), the effect of compaction effort in the measured resistivity is insignificant, which is discussed later in section 4.2.3 in more details.

Figures 21-23 represent the resistivity variation with water contents percent for the same soil specimens but measured immediately and 24 hours after removing the specimen from the oven. The solid lines with closed markers show the resistivity measured immediately after oven drying while the dashed lines with open markers indicate resistivity measured 24 hours after specimens' removal from the oven. As explained earlier, during these 24 hours, the specimens are stored in a plastic bag in the lab temperature in order to give the water inside the specimen the chance to equally distribute throughout the whole specimen (i.e., water content equilibrium). Results in Figure 4.3 indicate that measuring resistivity of the specimen immediately or 24 hours after oven drying gives approximately the same effect for the coarse sand type (soil passing No. 4 sieve). This conclusion is valid for all specimen tested from soil passing No. 4, regardless of the compaction effort used, as shown in Figure 21.

For fine grained sand (i.e., soil passing No. 16, and No. 50) results illustrated in Figures 22 and 23 indicate that water equilibrium through the soil specimen is significant for this type of soil. In addition, results in Figures 22 and 23 show that the resistivity measured after 24 hours is significantly higher than that measured immediately after oven drying, for the full range of water content used. This is because this time difference gave the water in pores the chance to equilibrate (i.e., distribute equally) throughout the soil specimens. As the soil gets coarser, the water in the voids equilibrates faster; therefore, soil passing No. 4 shows immediate resistivity that is very close to the 24 hours values. As the soil gets finer particles, such as sand passing No. 50 sieve, water in the pores takes time to reach equilibrium, and thus the immediate measured resistivity is much smaller compared to the 24 hours measured resistivity. More results are shown in Tables 7 through 25 in Appendix A.

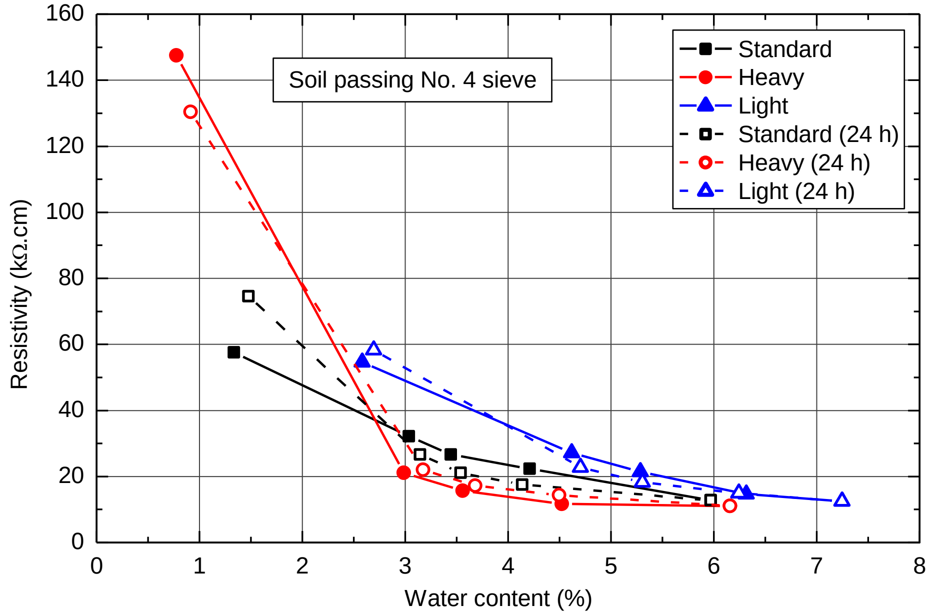

Figure 21: Variation of soil resistivity with water content for soil passing No. 4 sieve, tested immediately and 24 hours after oven dried

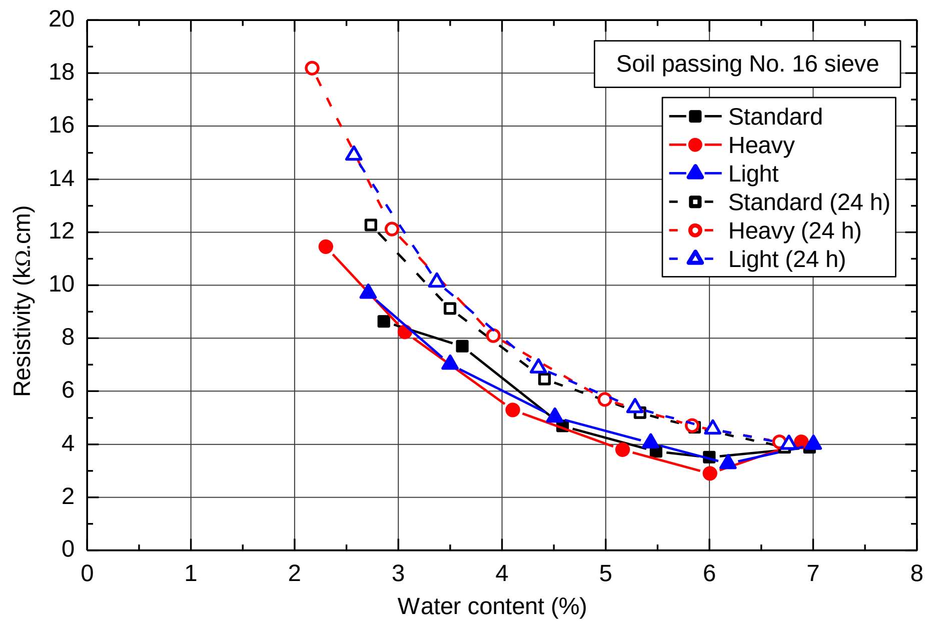

Figure 22: Effect of water content on soil resistivity for soil passing sieve no.16 both immediately and 24 h after drying

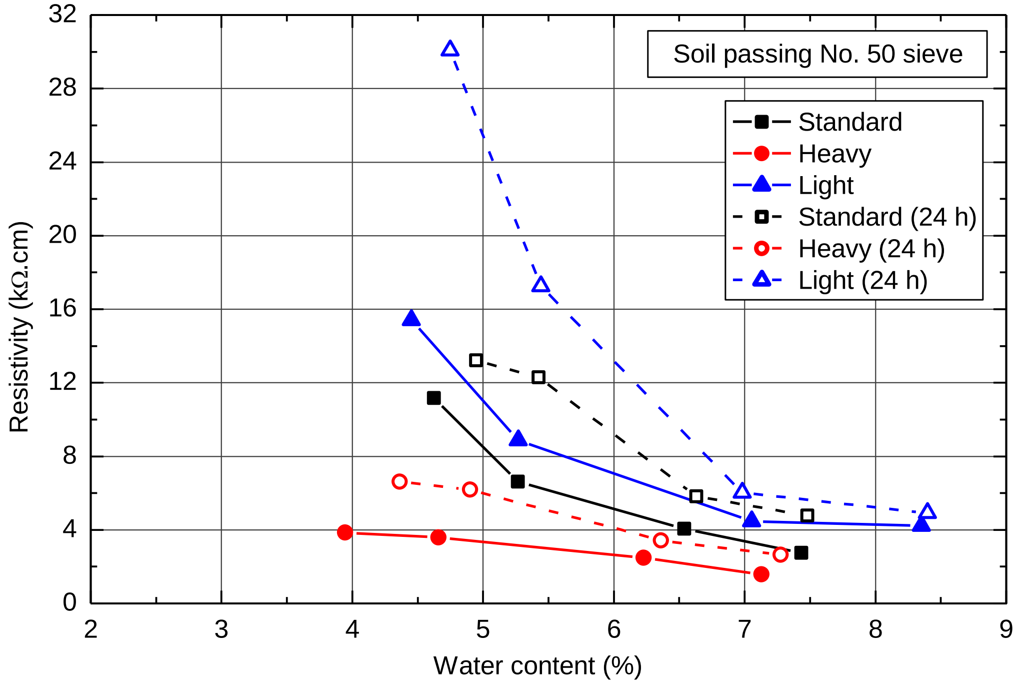

Figure 23: Effect of water content on soil resistivity for soil passing sieve no.50 both immediately and 24 h after drying

4.3.2 Effect of Soil Gradation on Resistivity. In order to study the effect of soil gradation (i.e., particle size distribution) on soil resistivity, three different gradations are made out of the original RAK soil by passing the soil through different sieve sizes. This sieving process results in the three soil gradations shown in Figure 19, with the same soil minerals. The soils are compacted with three different compaction efforts, namely: standard proctor, modified proctor and light compaction efforts. Soil passing No. 8 sieve is tested only at standard proctor compaction effort. Figures 24-26 show the effect of soil particle size distribution (i.e., gradation) on the resistivity variation with water content percent at different compaction effort. For all tests, resistivity was measured 24 hours after soil specimen was removed from the oven (that is, after water content equilibrium occurred). Results in Figures 24- 26 indicate that soil passing sieve No. 4 sieve (i.e., coarse sand) has the highest resistivity while soil passing sieve No.16 sieve (i.e., intermediate gradation soil) has the least resistivity at different water content and different compaction effort. This is expected as the fine sand (passing No. 16 sieve) has less void ratio compared to the coarse sand (passing No. 4 sieve), which means that particles are closer to each other in fine sand than coarse sand (i.e., more particles contact). In addition, at the same water content, the water in pores in soil with less void ratio is expected to have more continuity compared to the soil with large void ratio. Continuity or discontinuity of water in pores can be seen in Figure 27. It is well-understood that the soil with more particles contact and more pore water continuity would show less resistivity. Void ratio and particles contact are mainly affected by both compaction and gradation, as shown in Figure 28 (Das and Sobhan, 2014) [24].

As the sand gets finer than No. 16 sieve, such as in soils passing No. 50 sieve, Figures 24- 26 indicate that the resistivity of this soil is larger than intermediate finer/coarse soil (passing No. 16) but is still smaller than the resistivity of the coarse sand (passing No. 4 sieve). The resistivity increase in the soil passing No. 50 sieve indicates that one of the two factors affecting resistivity of soil (particle contacts and water connectivity) is reduced compared to soil passing No. 16 sieve. It is expected that particles points of contacts increase as the soil is gets finer, and hence this factor stays out of question. The remaining factor is the pore water continuity, which is highly affected with the soil gradation, and particles surface area. As the surface area of the soil particles increases, the amount of water required to saturate the surface areas of these particles increases. Therefore, water connectivity is expected to decrease in the case of finer sand (passing No. 50) compared to the intermediate finer sand (passing No. 16). These results in higher resistivity for soil passing No. 50 compared to soil passing No. 16.

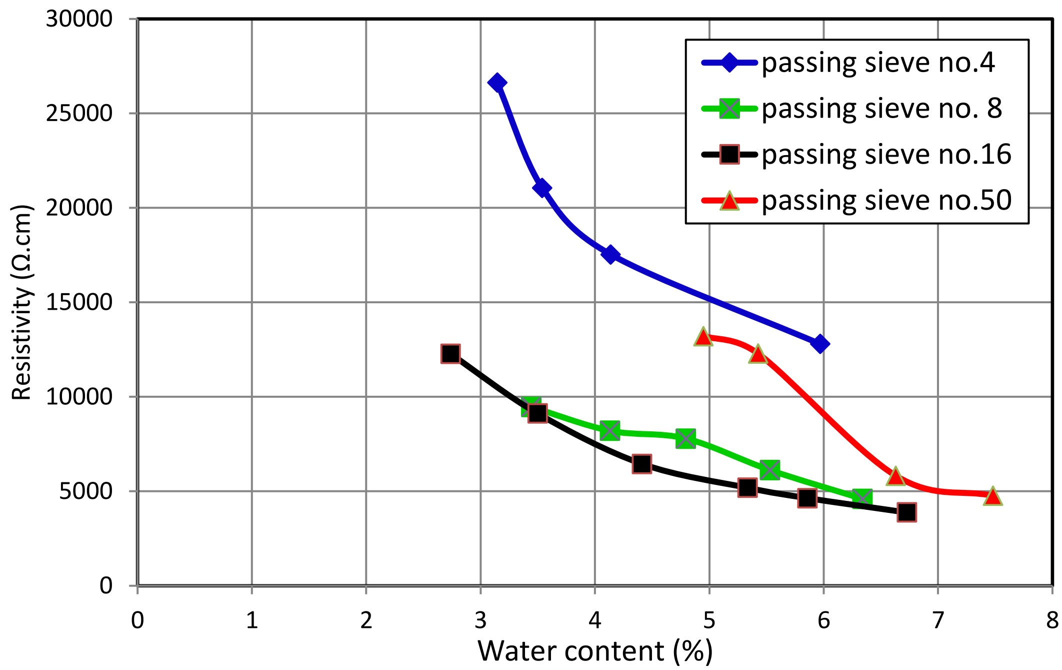

Figure 24: Variation of soil resistivity with gradation of soil compacted using standard compaction effort

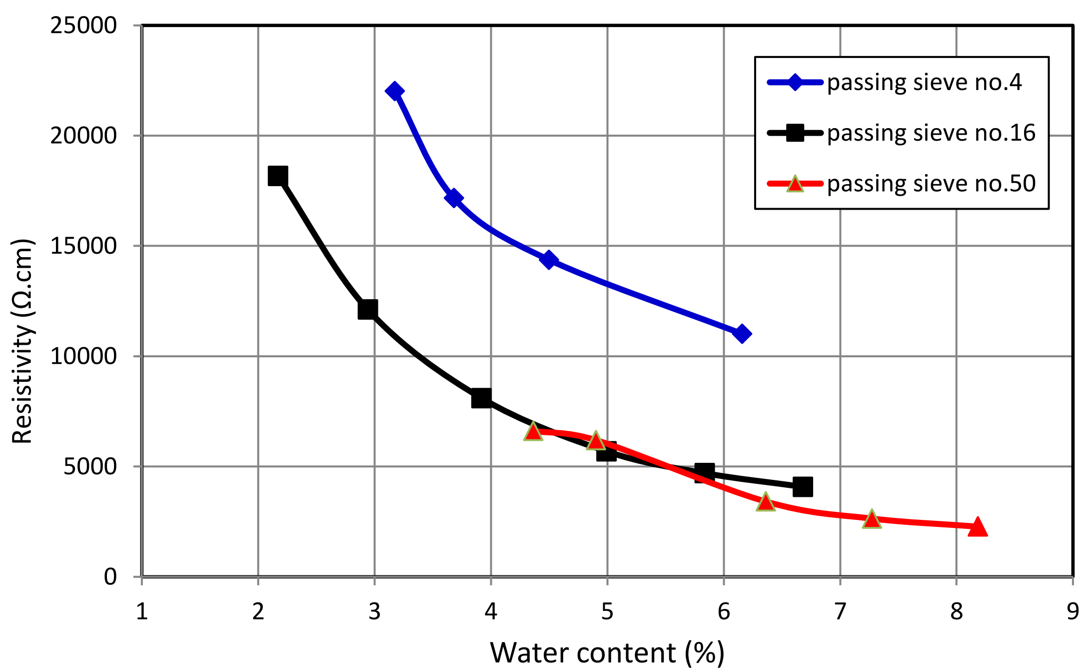

Figure 25: Variation of soil resistivity with gradation of soil compacted using heavy compaction effort

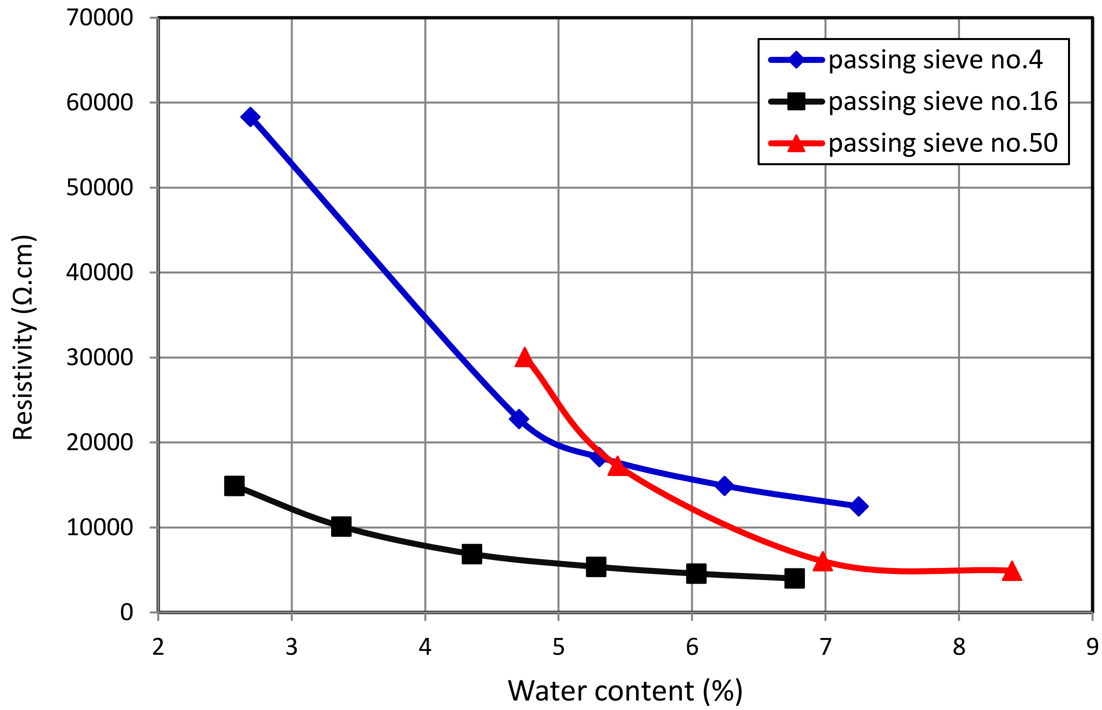

Figure 26: Variation of soil resistivity with gradation of soil compacted using light compaction effort

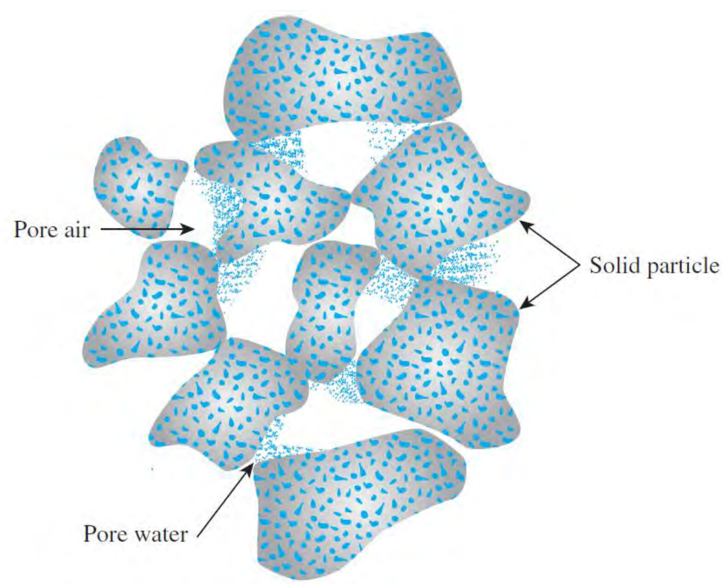

Figure 27: Pore water and water continuity in partially saturated soil (Das and Sobhan 2014) [24]

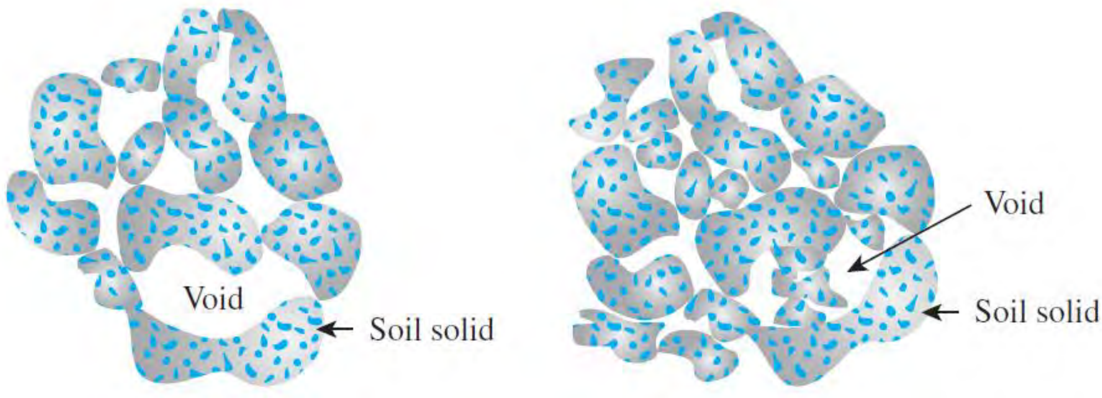

a) Sand with large void ratio b) sand with small void ratio

Figure 28: Particles arrangement and points of contacts for sand with large and small void ratio (Das and Sobhan, 2014) [24]

4.3.3 Effect of Void Ratio on Soil Resistivity. Variation of soil resistivity with void ratio at constant water content for two soils, passing No. 4, and passing No. 16 is shown in Figures 29 and 30, respectively. The resistivity is measured 24 hours after specimens are removed from the oven to allow water content equilibrium throughout soil specimens. As explained earlier, the two factors that affect soil resistivity are particles contacts and water connectivity. Particles contact points are decreased with the increase of the void ratio, so the resistivity increases, as shown in Figures 29 and 30. This variation of the soil resistivity with void ratio appears to be approximately linear in cases when water content equals 4% and 6%. However, as water content is reduced to 3%, a dramatic increase in soil resistivity occurs. At 3% water content, it can be seen from Figures 29 and 30 that the resistivity of the sand increases significantly when the void ratio increases beyond 0.77 and 0.65 for soil passing No. 4 and No. 16, respectively. Similar results are found by Fallah-Safari et al. (2013) [16]. More results are shown in Tables 7 through 25 in Appendix A.

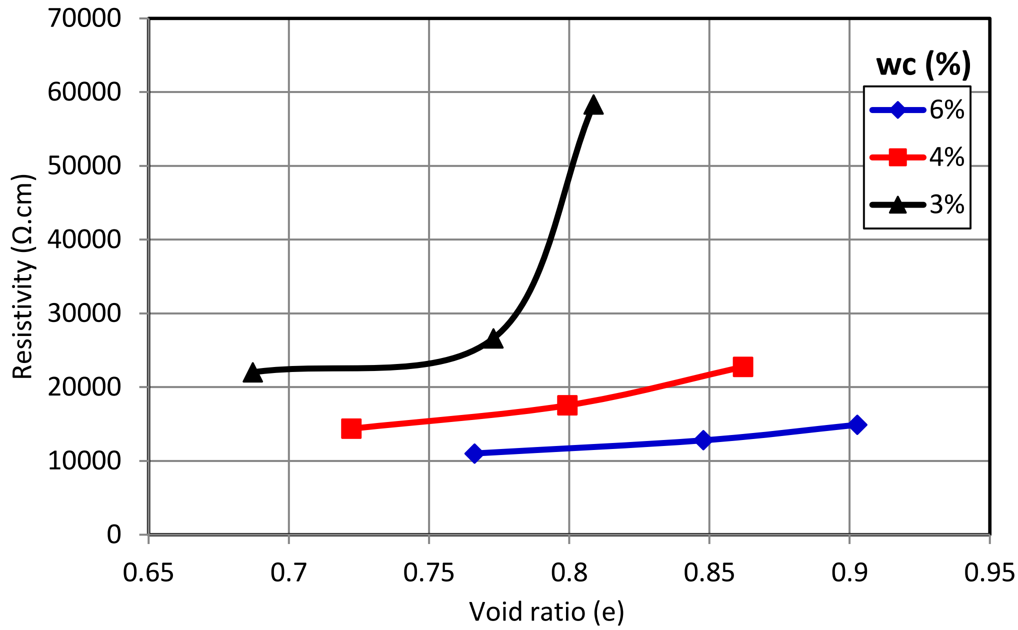

Figure 29: Variation of soil resistivity with void ratio (e) at different water contents, for soil passing No. 4 sieve (24 hours after drying)

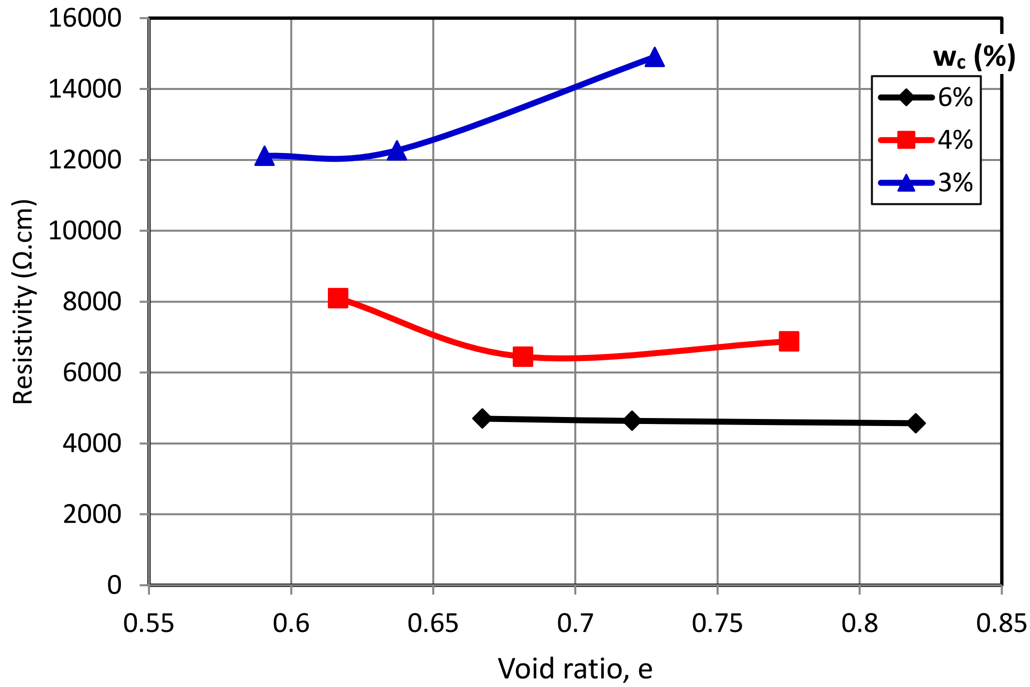

Figure 30: Variation of soil resistivity with void ratio (e) at different water contents, for soil passing No. 16 sieve (24 hours after drying)

4.3.4 Effect of 24 hour water content equilibrium time. To study the effect of water equilibrium and distribution on the measured resistivity of the tested soil, the resistivity was measured twice on the same sample at approximately same water content percent. A resistivity measurement was taken immediately after the soil specimen was removed from the oven, and a second measurement was taken 24 hours after specimen removal from the oven. During these 24 hours, the specimen was stored in plastic bag which tightly sealed and given the chance for the pore water to re-distribute evenly among all points of the specimen. It was expected that the parts of the specimen that are closer to the surfaces to be over-dried while the inner parts to be under-dried. The under-dried regions will have larger water content and may be more water continuity compared to the under-dried regions. Therefore, the under dried regions will have small resistivity, and the over dried regions will have high resistivity, and the overall resistivity of the specimen will depend on the relative volume of these regions. Keeping the specimen for 24 hours in a water tight bag is re-distributing the water from areas with larger water content (under-dried areas) towards areas of lower water (over-dried areas). Figure 31 show that this process significantly affected the measured resistivity of the sandy soil. It can be seen from Figure 31 that the resistivity measured after 24 hours of drying is much larger than its measurement immediately after drying. This is due to the re-distribution of pore water through the soil specimen which may result in some pore water discontinuities. Water discontinuities are a major reason for increasing soil resistivity.

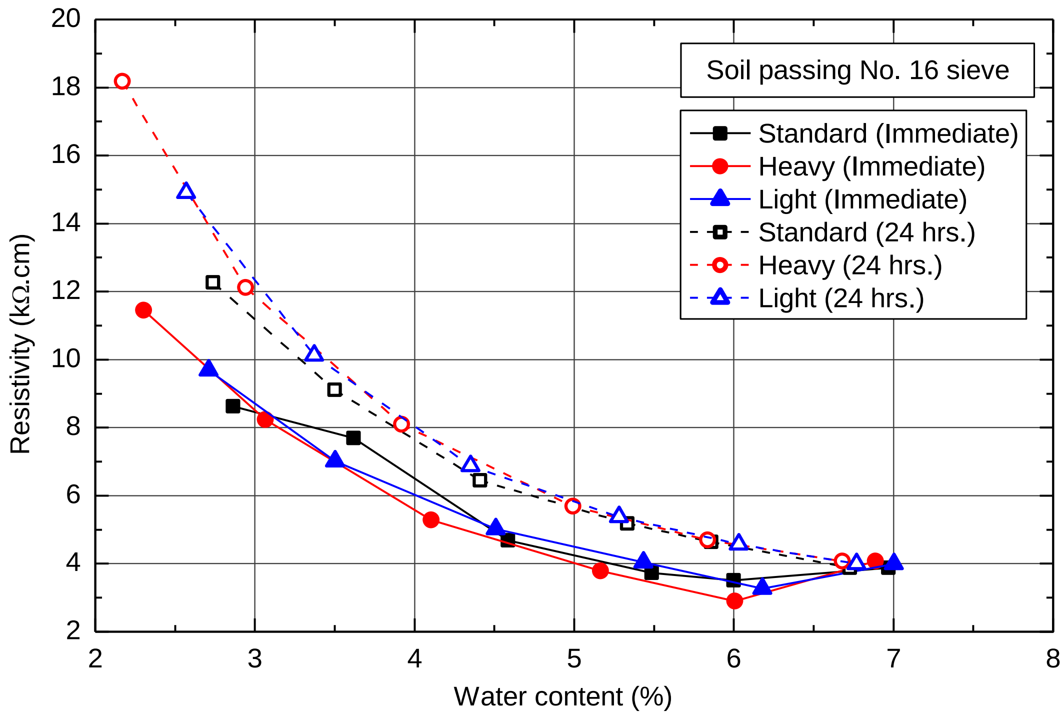

Figure 31: Effect of water content on soil resistivity for soil passing sieve no.16 both immediately and 24 hours after drying

4.2.5 Effect of Clay Content on Soil Resistivity. To study the effect of clay content on the resistivity variation, different percentages of clay contents have been mixed with soil passing No. 16 sieve in order to obtain sand dirty with clay. Clay contents of 10%, 20% and 30% by weight of dry sand have mixed with the sand, and then mixed with the required water content percent to be compacted in the standard proctor mold. The resistivity was measured 24 hours after the specimen removed from the oven for the water content equilibrium. Figure 32 shows the variation of resistivity versus water content percent at different clay contents. While Figure 33 compares the effect of clay contents at similar water content percent. It could be noticed from Figure 32 that the soil with 10% clay content has the lowest resistivity at the water content range used in this study. In addition, up to 8.4% water content, the soil with clay content equal to 30% shows the largest resistivity. As the water content increased beyond 8.4%, the resistivity of sand with 30% clay content becomes lower than that for the sand with 20% clay content. Individual clay soil has lower resistivity compared to sand and rock; however, results in Figure 32 indicate that the addition of clay increased the soil resistivity. The reason for that is the absorption of pore water by clay content which causes a significant effect on the soil resistivity. In reality, clay blocks the pores of the sandy soil in a process called "Lithification", and absorb the pore water, leaving the sand particles with no water around it. This process destroys the geometrical connectivity of pore water inside the soil, which is the major factor affect resistivity. In fact, if clay is added to sand in a dry condition, the resistivity should be decrease, however, in these tests water content almost higher than 5%. The existence of the clay together with high water content is expected to act differently compared to the existence of the clay in dry soil. This explains why the resistivity of sand increased if clay is added with certain percentage. Similar results were found by Fallah-Safari et al. (2013) [22].

For the sand soil that contains 30% clay, Figure 32 indicates that the resistivity becomes lower compared to the sand with 20% clay content when water content increases beyond 8.4%. This could be due to the formation of continuous wet clay matrix through the sandy soil spacemen. This occurs only when the clay content is large to overflow outside the voids and when the water content is high enough to form the electrical double layer at the interface of the clay mineral and the water. This effectively allows ions to move through the system with a higher mobility than in the liquid phase (i.e., reduces resistivity). Figure 33 indicates that, at the same water content percent, the resistivity increases with clay content and specifically decreases at 30% clay contents. The only exception of that is the resistivity at water content equal to 7.5% where the resistivity increases with clay content percent without showing any decrease at higher clay content. More results are shown in Tables 26 to 28 in Appendix A.

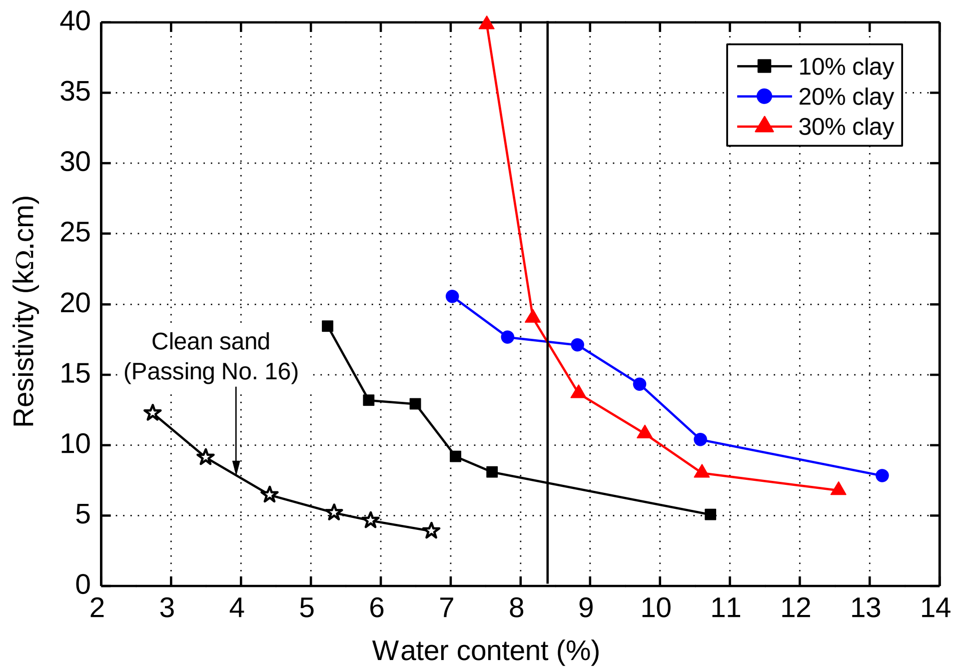

Figure 32: Variation of soil resistivity versus water content at different clay content

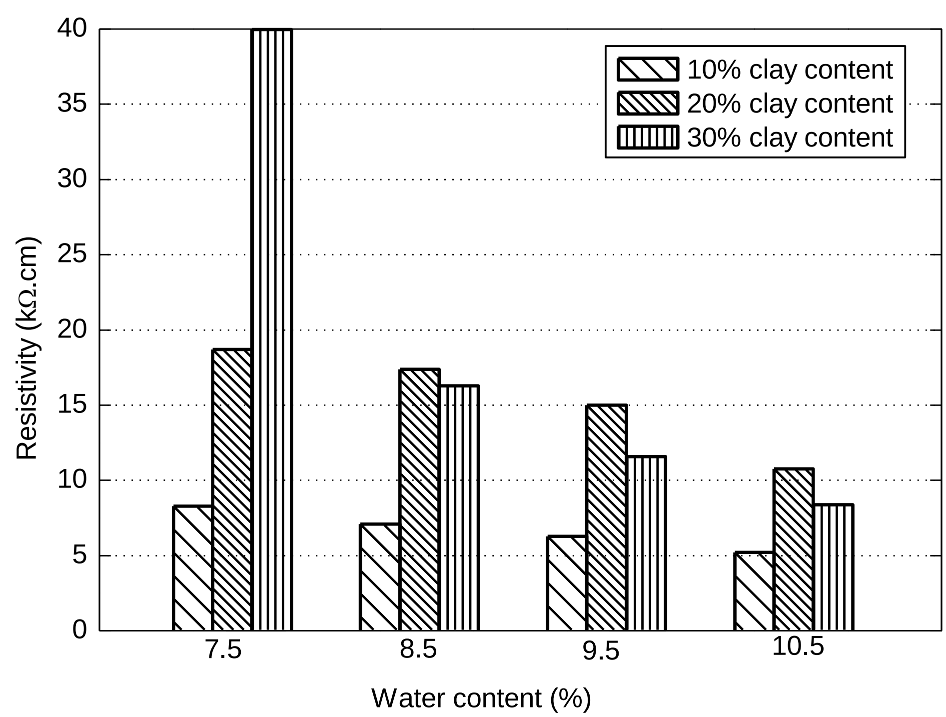

Figure 33: Variation of soil resistivity with clay content at different water content

4.4 Results of GPR Application

This section presents and discusses results from GPR tests that are used to measure the dielectric constant at different water contents for two different soil types. As stated earlier, two different soil types have been tested using GPR; the first one (soil_1) is the original RAK soil or the soil passing No. 4 sieve while the second soil (soil_2) is a modified gradation of the first one by passing it on the sieve No. 8. In addition, example results of the direct shear tests that are conducted on all soil types are also presented. Finally, an extensive regression analysis that is conducted to relate different soil parameters in a practical and usable approach is discussed.

4.4.1 Dielectric Constant of Soil_1. Following the procedures discussed in section 3.3.1, the dielectric constant of soil_1 is measured at different water content percent and different compaction. Table 29 shows the measured dielectric constant of soil_1 at different water content while Figures 34-39 show the scanned soil pictures using GPR at different water contents and different compaction.

Table 29: Dielectric constant and water content percent of soil_1

Water Content %	Compacted	Dielectric Constant	Figure No.
0.00	yes	4.0	34
2.68	yes	5.5	35
3.30	yes	6.5	36
5.40	yes	8.0	37
7.68	yes	8.8	38
7.68	no	9.0	39

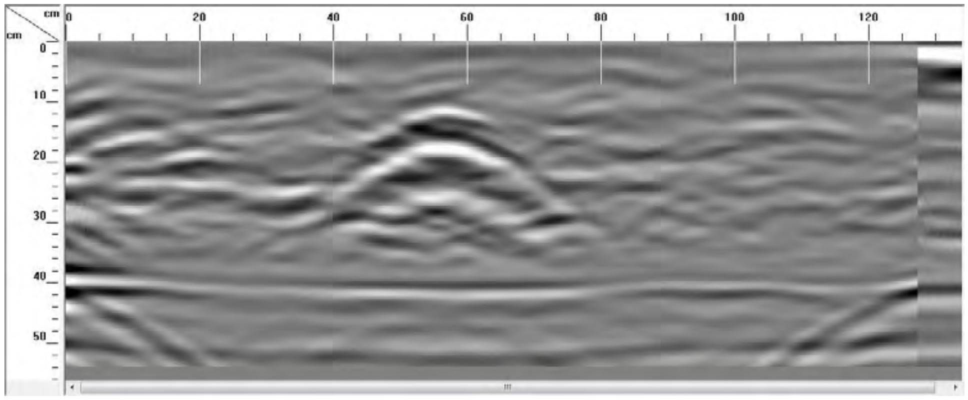

Figure 34: Water content 0.00 %, with compaction, dielectric constant 4.0

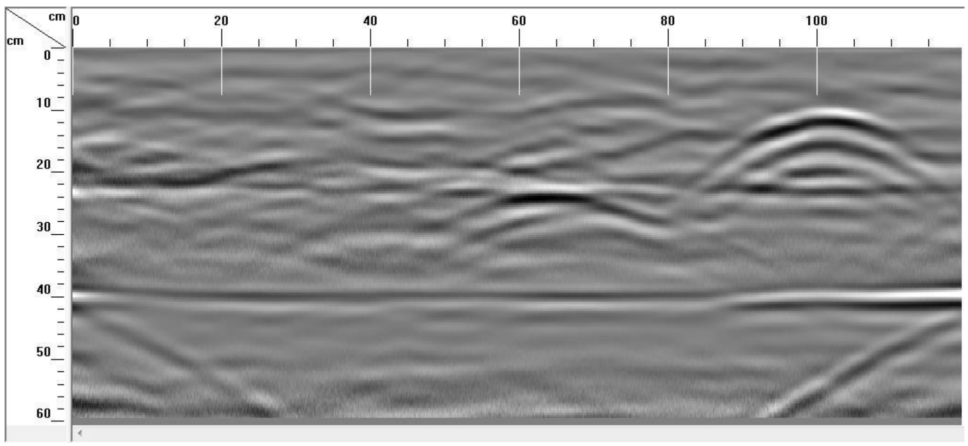

Figure 35: Water content 2.68 %, with compaction, dielectric constant 5.5

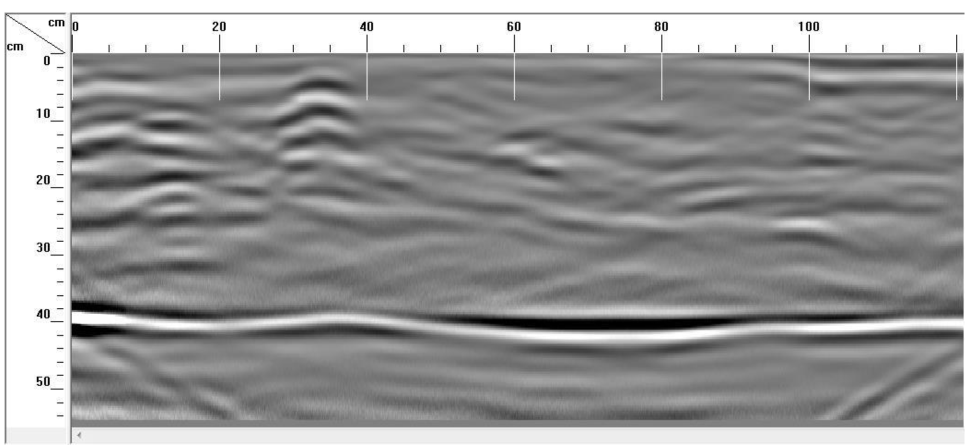

Figure 36: Water content 3.30 %, with compaction dielectric constant 6.5

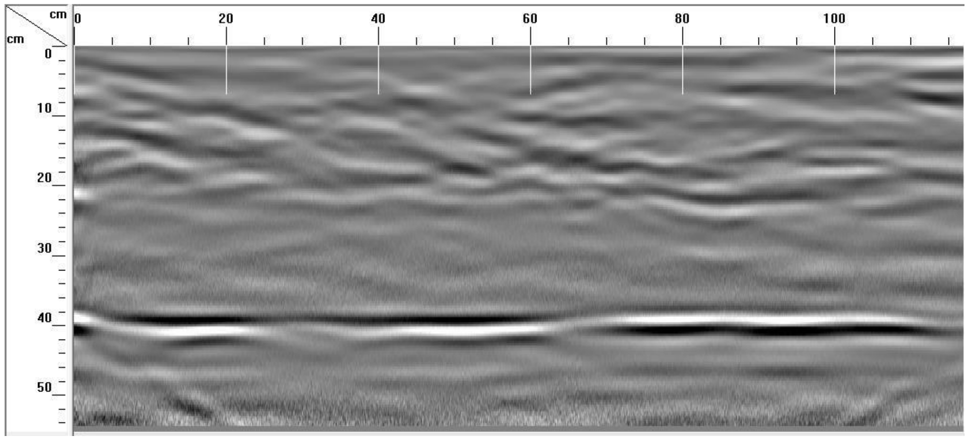

Figure 37: Water content 5.40 %, with compaction, dielectric constant 8.0

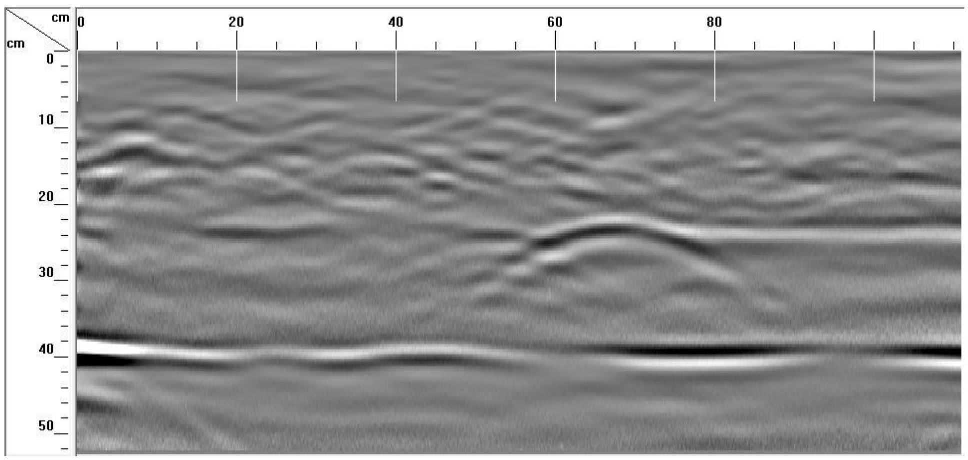

Figure 38: Water content 7.68 %, with compaction, dielectric constant 8.8

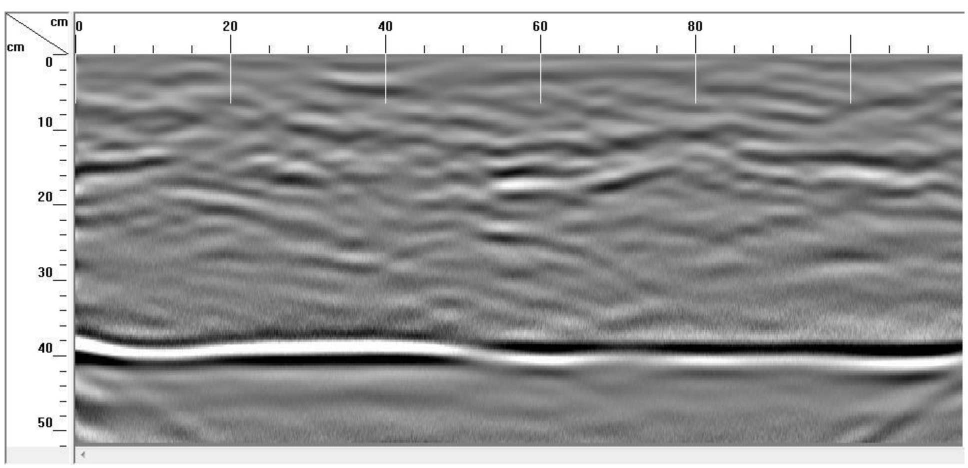

Figure 39: Water content 7.68 %, without compaction, dielectric constant 9.0

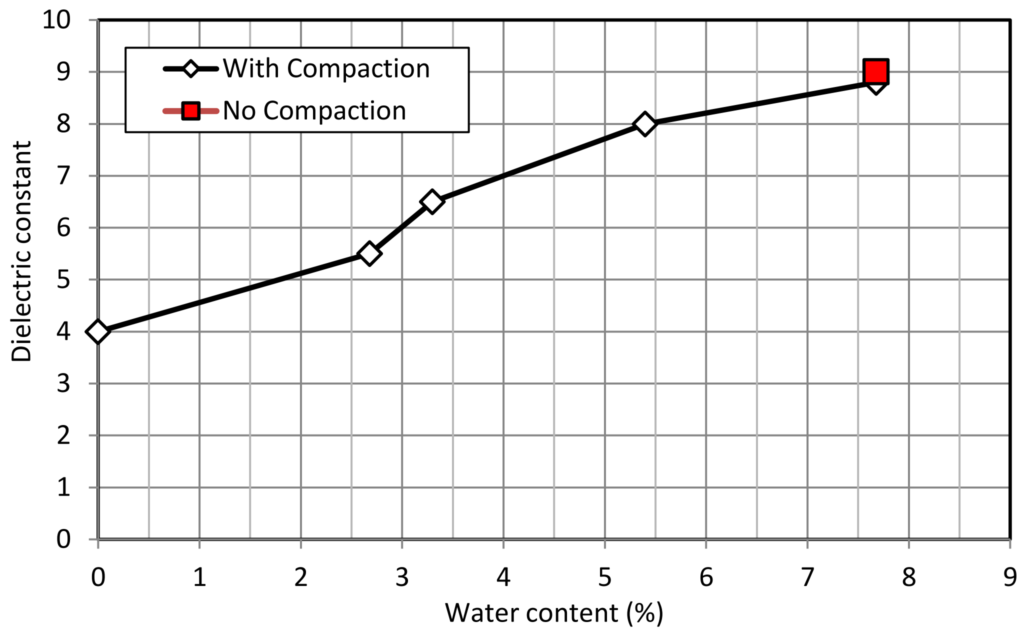

Figure 40: Variation of soil_1 dielectric constant with water content percent and the effect of compaction effort

Variation of soil_1 dielectric constant versus water content percent is shown in Figure 40. The figure also demonstrates one test that is repeated at 7.7% water content but without any soil compaction. This test is conducted to investigate the effect of compaction effort on the soil dielectric constant. It should be noticed that un-compacted dielectric constant test is only one test, and its results need to be used with caution. Results in Figure 40 indicate that the soil dielectric constant increases as the water content of the soil increases. In addition, the test conducted with loose soil gives a dielectric constant similar to the compacted test at the same water content percent. Finally, the dielectric constant at 5.4% water content is almost double its value for the dry soil. More results are shown in figures 41 to 44 in Appendix B.

4.4.2 Dielectric Constant of Soil_2. Soil_2 is the soil modified from RAK original soil (soil_1) by sieving it on NO. 8 sieve. This soil is also subjected to the application test using GPR to measure its dielectric constant at different water contents. Table 30 shows the measured dielectric constant of soil_2 at different water content. While Figures 45-50 show the scanned soil pictures using GPR at different water contents and different compaction.

Table 30: Dielectric constant and water content percent of soil_2

Water Content %	Compaction	Dielectric Constant	Figure No.
0.00	yes	4.0	45
1.57	yes	4.8	46
4.01	yes	6.2	47
5.34	yes	8.5	48
8.74	yes	10.0	49
8.74	no	8.9	50

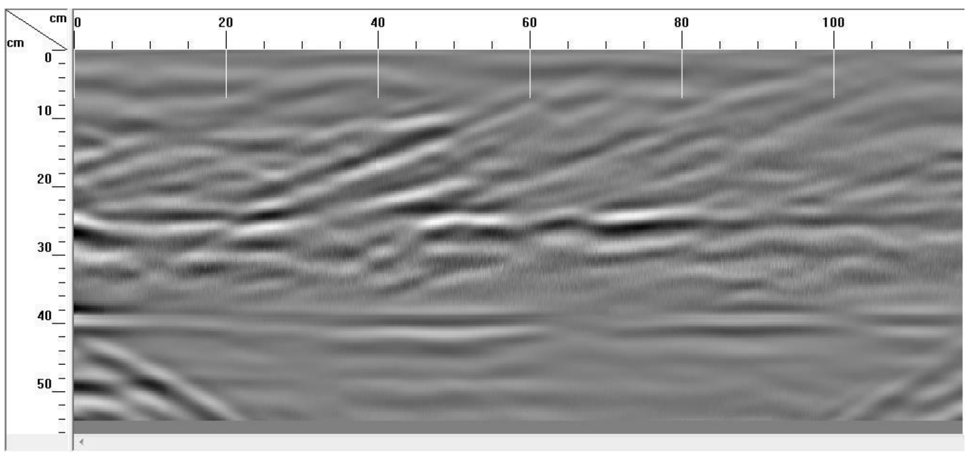

Figure 45: Water content 0.00 %, with compaction, dielectric constant 4.0

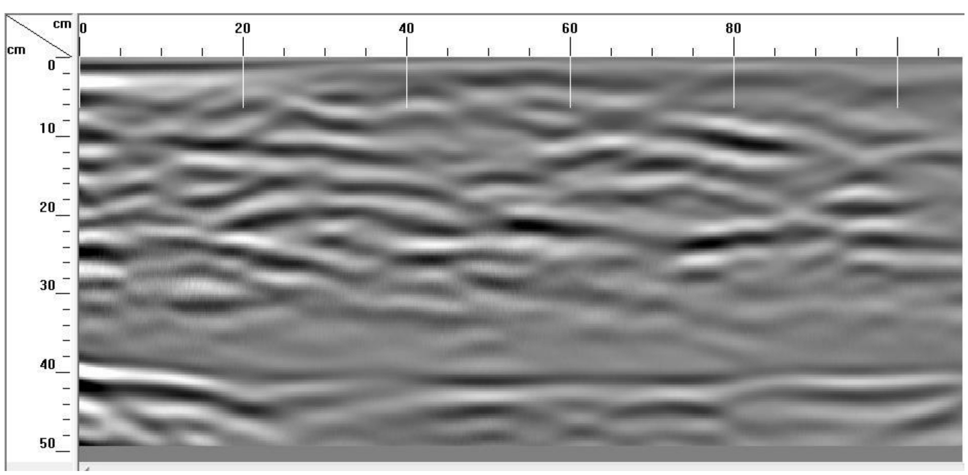

Figure 46: Water content 1.57 %, with compaction, dielectric constant 4.8

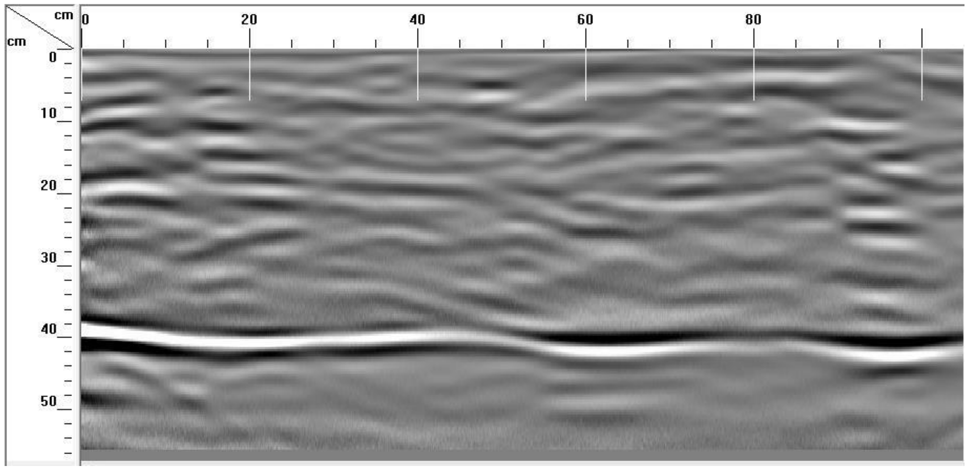

Figure 47: Water content 4.01 %, with compaction, dielectric constant 6.2

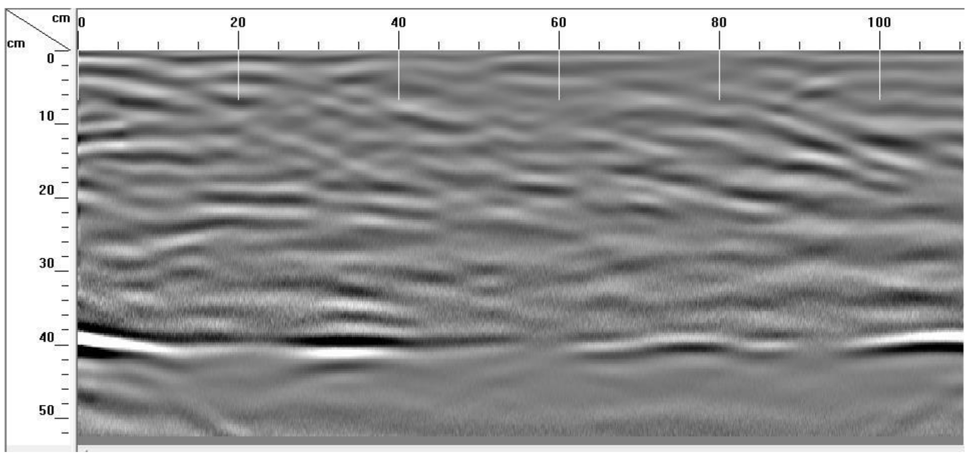

Figure 48: Water content 5.34 %, with compaction, dielectric constant 8.5

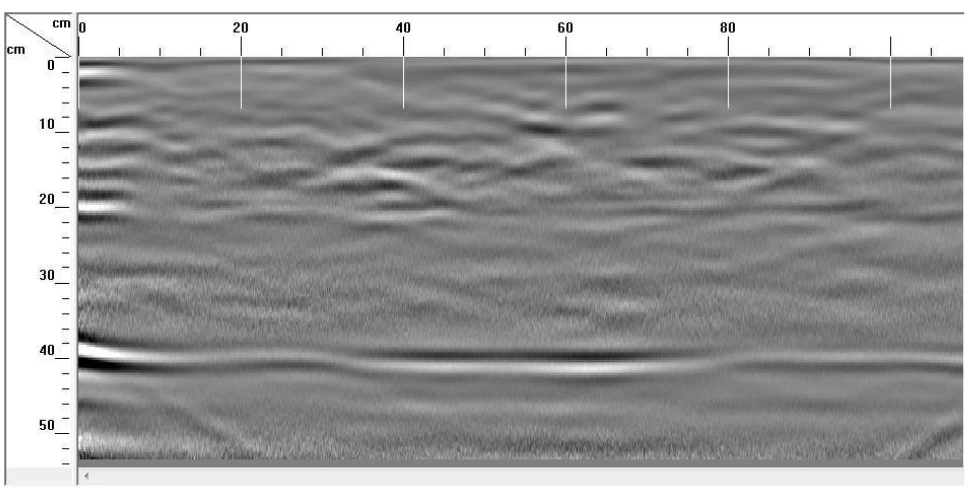

Figure 49: Water content 8.74 %, with compaction, dielectric constant 10.0

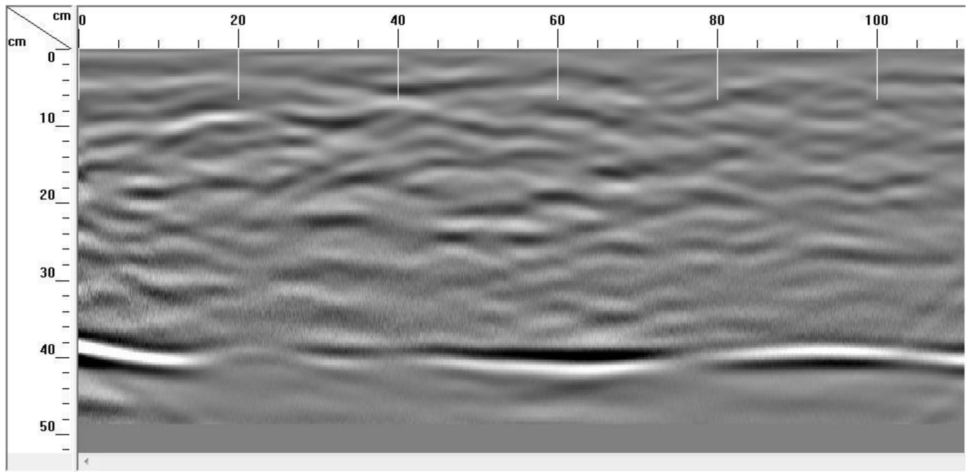

Figure 50: Water content 8.74 %, without compaction, dielectric constant 8.9

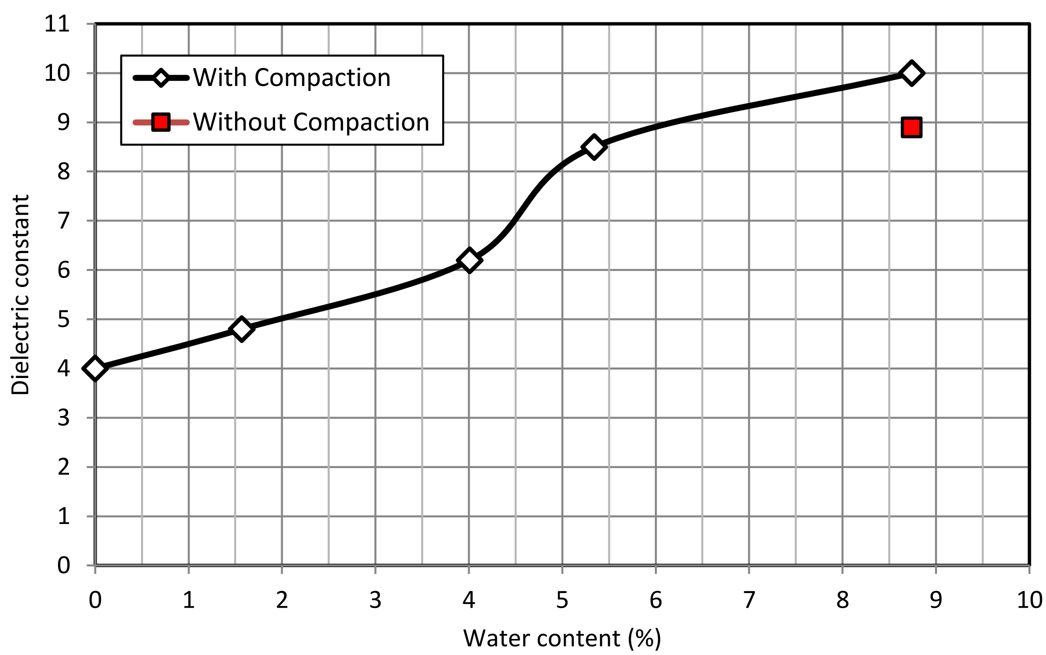

Figure 51: Effect of water content and compaction on dielectric constant of soil_2

Variation of soil_2 dielectric constant versus water content percent is shown in Figure 51. Figure 51 also presents the value of dielectric constant from one test repeated at

8.7% water content, but with no compaction (loose soil). The purpose of this is to isolate the effect of compaction effort on the measured dielectric constant. Once again, this test should be used carefully as it is only one test. Results in Figure 51 indicate that the soil dielectric constant of soil_2 increases as the water content increases. In addition, the test conducted with loose soil gives a dielectric constant slightly smaller compared to the compacted test at the same water content percent. Finally, the dielectric constant of this soil at 5.4% water content is almost double its value for the same dry soil.

4.4.3. Example Direct Shear Test Results. Direct shear tests have been conducted on all soil types used in this research work in order to measure the internal friction angle of different soil types. A number of 40 different soil specimens has been prepared and tested in the AUS direct shear setup. These samples are prepared at different water content percent and tested at different normal stresses (σ_n). Shear stresses versus horizontal deformations are measured for each tested specimen. Example of shear stress versus horizontal deformation for soil_1 tested at normal stress σ_n = 55 kPa in dry condition is shown in Figure 52. Figure 53 shows the resulted friction angle for soil_1 which is about ϕ = 40° at 5.8% water content. More results are shown in Table 31 in Appendix C.

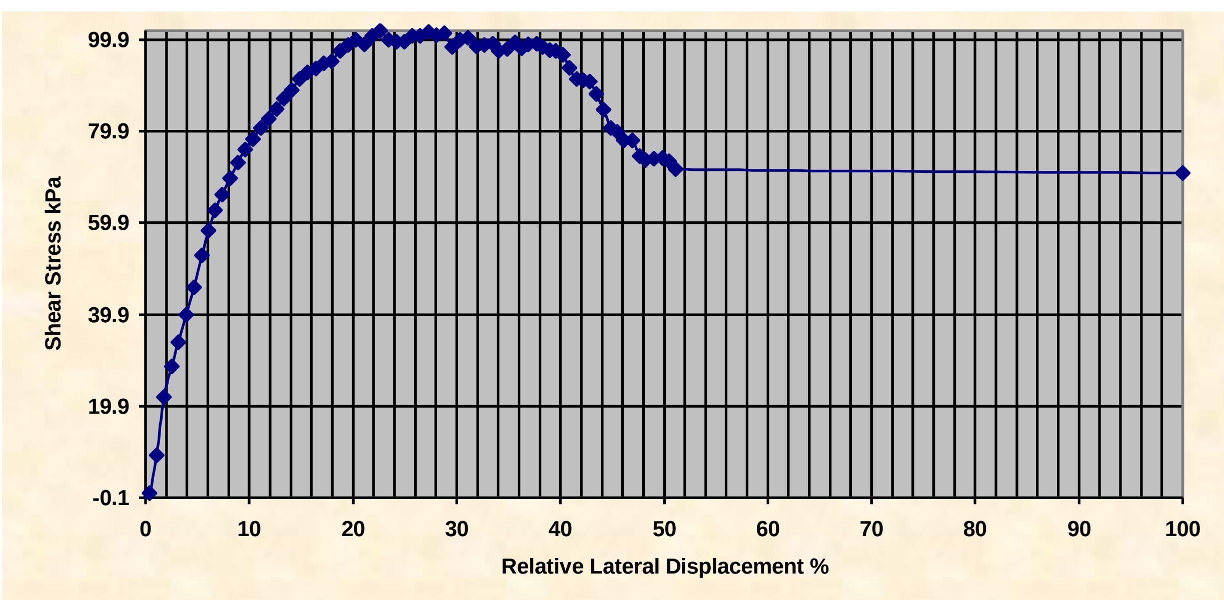

Figure 52: Shear stress versus horizontal deformation for soil_1, at normal stress σ_n = 55 kPa

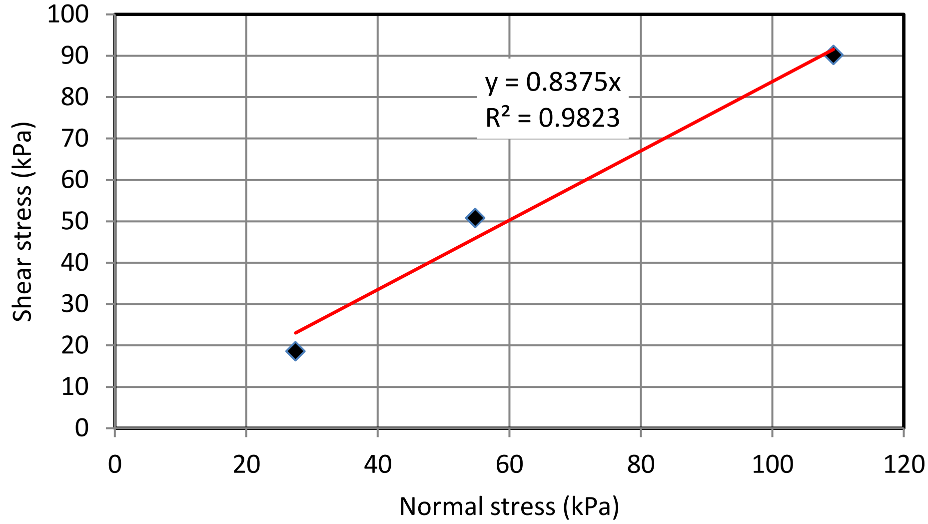

Figure 53: Friction angle for soil_1 at about 5.8% water content

Chapter 5: Implementations of the Test Results

5.1. Data Interpolation and Regression Analysis

In order to relate different soil parameters to the dielectric constant measured using GPR, an extensive regression and data interpolation have been conducted. Through this analysis, soil parameters that are measured in the lab, such as direct shear friction angle is related to the resistivity which is measured using index tests, and finally related to the dielectric constant which is measured using GPR application. It should be kept in mind that the ultimate goal of this research work is to predict soil parameters using GPR. Therefore, the purpose of this section is to relate the measured soil friction angle and void ratio to the dielectric constant.

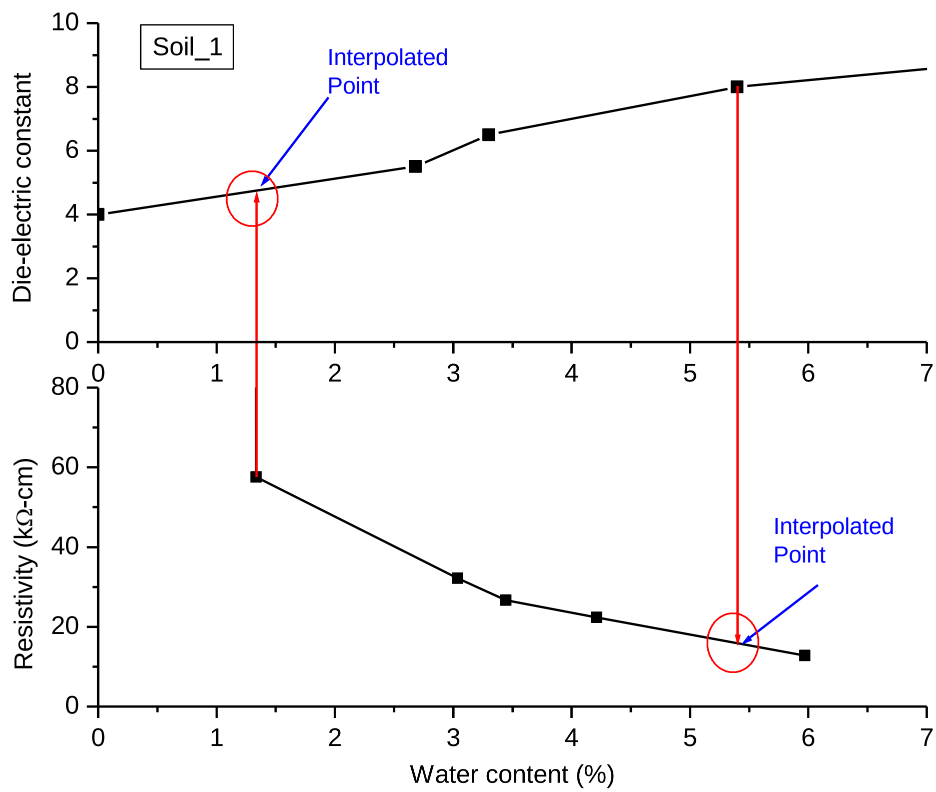

Figure 54: Interpolation process for soil_1 (Passing No. 4 sieve)

The analysis starts with data interpolation of both soil resistivity and dielectric constant at similar water content percent. This allows the relationship between soil resistivity and dielectric constant to be established. The interpolation process is presented in Figures 54 and 55 for both soil_1 and soil_2, respectively. Basically, values of resistivity are interpolated at water contents associated with the dielectric constant values measured using GPR, and the dielectric constant is interpolated at values of water content associated with the resistivity values measured at index tests.

Results of interpolation are relationships between soil resistivity and soil dielectric constant, as shown in Figure 56. Regression analyses have been conducted using Microsoft Excel to get the best fit equation with the highest Correlation coefficient (R^2), for both soil types. In the regression process, the power equation was found to fit both data in a good correlation as shown by $R_1^2 = 0.976$, and $R_2^2 = 0.803$. It can be seen that the power equation correlates the measured data of soil_1 better than the correlation of soil_2. The resulted correlation equations based on this regression analysis are as follow:

$$R = 3000\, \xi^{-2.545} \quad \text{……………………………………Eq 6.}$$

$$R = 4000\, \xi^{-3.089} \quad \text{……………………………………Eq 7.}$$

Equations 6 and 7 are established for soil_1 and soil_2, respectively to calculate the soil resistivity R in kΩ-cm based on the dielectric constant ξ measured using GPR. Therefore, practically, instead of measuring soil resistivity on the site, practitioners can use the GPR to measure the soil dielectric constant and calculate the soil resistivity using Equations 6 or 7 depending on the soil type and gradation. It is well-known that the logistic, the time consumption and easiness are on the side of GPR compared to the resistivity test.

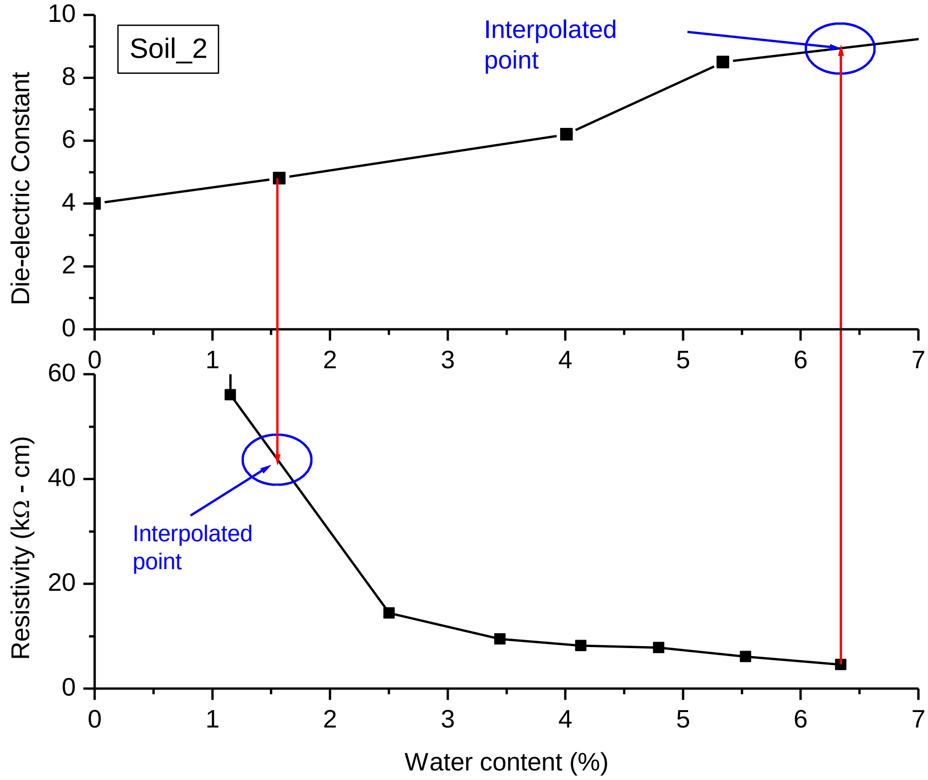

Figure 55: Interpolation process for soil_2 (Passing No. 8 sieve)

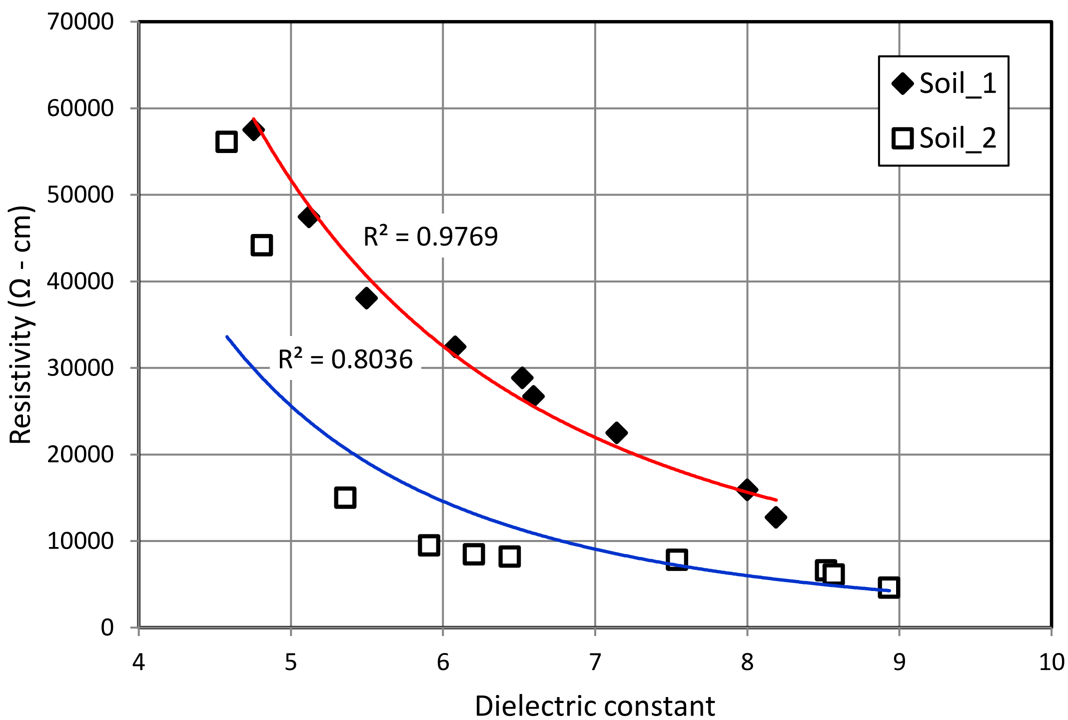

Figure 56: Interpolation outcomes for soil_ and soil_2 with the best fit equations and their correlation coefficients

5.2. Three-Ways Implementation Graph

Results of interpolation and regression analyses and relations between resistivity and water content percent that are established in index tests together with the direct shear test results are used to create a 3-ways graph as shown in Figure 58. The 3-ways graph can be used to deduce the soil friction angle from the measured dielectric constant of the soil in 3 steps. The blue colored arrows explain the directions of movement throughout the graph, the start point to get into the graph, and the end point to deduce the soil friction angle "Explanation Steps". Different equations presented in Figure 58 are shown in Table 32, where R is resistivity in kΩ-cm, ϕ is friction angle in degrees, and w_c is water content as a percentage.

5.3. Verification Tests

Verification tests have been conducted on the original RAK soil (passing sieve No.4.). Dielectric constant is measured in the site using GPR as illustrated in Figure 57, while friction angle is measured in the lab by direct shear test for the same soil sample, and at the same water content percent. Results of these tests render a dielectric constant $\xi = 7.3$, and friction angle $\phi = 41°$, at water content percent $w_c = 4.3\%$. Using Figure 58 and a value of dielectric constant $\xi = 7.3$, the graph can be interred with the upward black vertical arrow to cut the curve of soil_1. Then, designer moves horizontally to the right with horizontal black arrow to cut the curve of resistivity-water content relation of soil_1. Thereafter, move downward with the black arrow to cut the curve related the friction angle of soil_1 to the water content.

Table 32: Regression equations for resistivity and friction angle as functions of water content

Equation	R^2	Soil type	Units	Eq. No.
$R = 91.4w_c^{(-1.013)}$	0.9538	Soil_1	R = kΩ - cm w_c = %	(4)
$R = 69.2w_c^{(-1.466)}$	0.9772	Soil_2		(5)
$\phi = 55 - 4.8w_c + 0.38w_c^2$	1	Soil_1	ϕ = degrees w_c = %	(6)
$\phi = 52 - 5.4w_c + 0.52w_c^2$	1	Soil_2		(7)

Figure 57: Using the GPR to determine the Dielectric constant in site

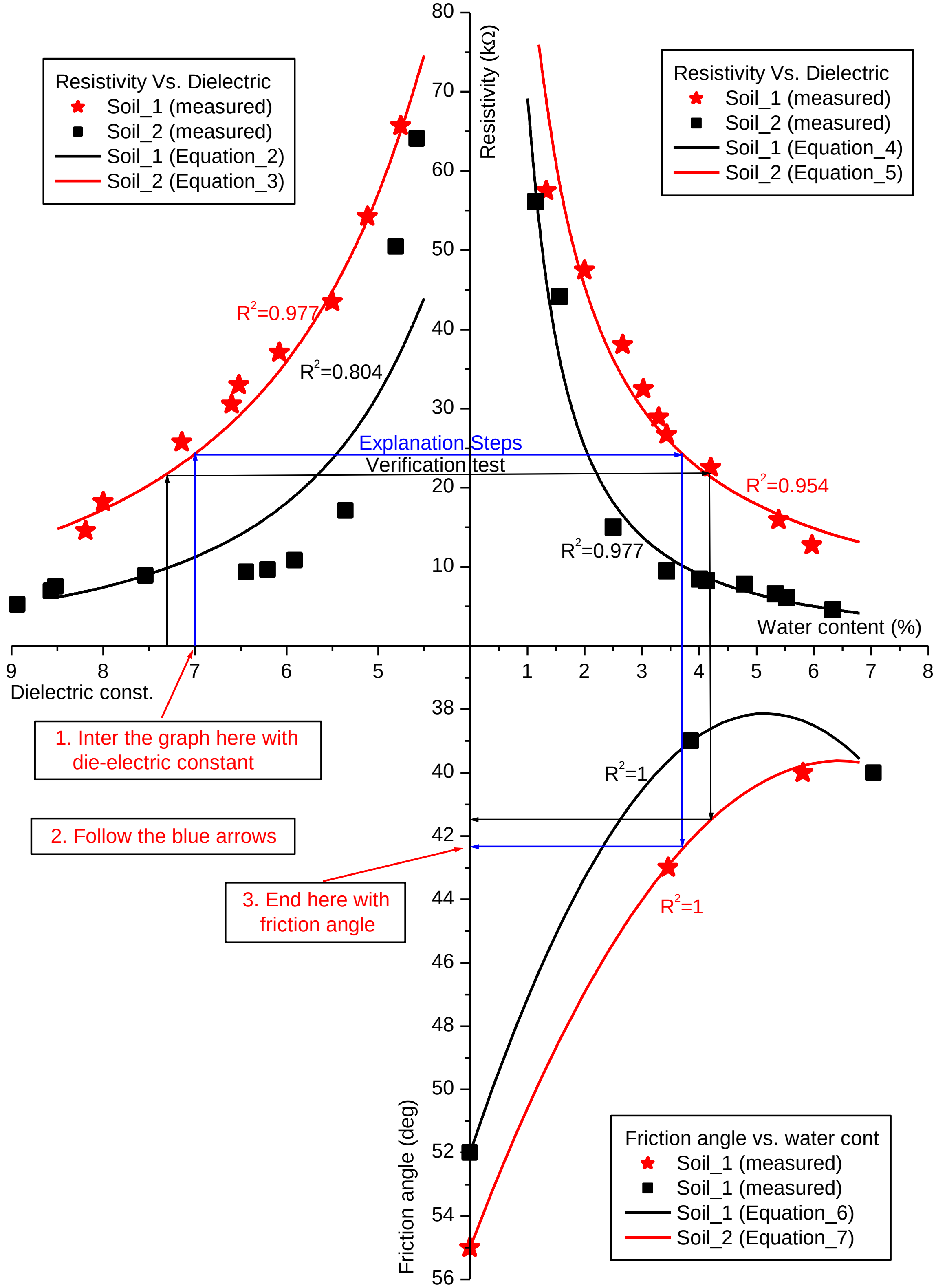

Figure 58: Three-ways graph for soil_1 and soil_2

Chapter 6: Conclusion and Recommendations for Future Work

6.1 Conclusion

In this study, a number of 200 index tests have been conducted in the American University of Sharjah geotechnical lab. Different sandy soil samples with different gradations were tested to study and relate the resistivity of the soil with different water contents, void ratios, compaction efforts, clay contents and friction angles. Thus, samples are prepared inside the standard proctor molds, using modified hammer. In addition, direct shear tests have been conducted to investigate the variation of peak friction angle with the water content percent for all soil types used in the index tests. The following important points can be summaries from these index tests:

1. Generally, soil electrical resistivity decreases (i.e. conductivity increases) as the soil water content increased. This is true for all soil types tested in this research, regardless of the compaction effort, soil type, and time allowed for water content equilibrium.
2. For the same type of soil, and same water content/degree of saturation, soil resistivity decreases as the compaction effort increases, as heavy compaction increase particle and water connectivity/continuity.
3. The sandy soil with fine gradation is highly affected with the compaction effort compared to the sandy soil with coarse gradation.
4. Coarse grained sand shows the highest resistivity, while soil passing sieve No.16 sieve (i.e. intermediate fine gradation soil) has the least resistivity at different water content and different compaction effort.
5. Particle contact points are water connectivity decreases with the increase of the void ratio and therefore, the resistivity increases.
6. For dry sand, the addition of clay is expected to reduce resistivity, while for wet sand the addition of clay increases the soil resistivity.
7. The soil friction angle decreases as the water content percent increases, for all sand soil tested in direct shear tests.

8. For extremely hot withers like UAE, it is recommended for the in-situ resistivity measurement to be conducted early in the morning to allow for the soil water content equilibrium which might be disturbed during a long hot-sunny day.

Field tests application using GPR are performed to study the behavior of the dielectric constant of two different types of sandy soil; original RAK soil passing sieve No. 4 and modified RAK soil passing sieve No. 8. The main difference between the two different soils is the grain size distribution. In addition, water content is varied between different tests. The following points can be concluded from the GPR tests:

1. The soil dielectric constant increases as the water content increase, which is opposite to the resistivity variation with the water content for the same soil type.
2. Combining the index and the GPR tests resulted in exponential relationships between soil dielectric constants and resistivity, with near perfect correlation coefficient.
3. A three-step graph was developed to relate soil friction angle which measured in direct shear tests to the soil dielectric constant which measured on site through soil resistivity, which is well established in literature and measured in the current study.
4. The three-step graph shows similar trends for both soil types despite the different grain size distribution curves for both soils.
5. A level-A prediction test have been conducted and shows perfect matches with values predicted using the developed three-steps graph.

6.2 Recommendations for Future Research

The advancement in technology has made it easier for geotechnical engineers to come up with new alternatives to the conventional time consuming and cost inefficient tests. This research is in the area of using the GPR, a nondestructive technique, in order to predict the friction angle of the sandy soil in the field without the need of using conventional lab test, such as the direct shear test. This research study the applicability of GPR to predict the friction angle for only two types of soil: Original RAK soil passing sieve NO. 4, and

Modified RAK soil passing sieve No. 8. The following points can be recommended for future work:

1. This research needs to be extended to study other soil gradation of the same soil type, in order to have more curves on the three-way graph.
2. GPR tests for the other two soil gradations tested in index tests (passing No. 16 and No. 50) need to be conducted, which allows another 2 sets of curves added to the 3-steps graph.
3. Other ranges of water contents and degree of saturations could be investigated for the same soil types used in this study.
4. Different sandy soil types other than the types tested in this research can be tested to generalize the current results.
5. Different soil parameters, other than soil friction angle, such as soil permeability and void ratio, could be related to the soil dielectric constant.

References

[1] Turesson A. “Water content and porosity estimated from ground penetrating radar and resistivity.” *Journal of Applied Geophysics*, vol. 58, pp. 99-111, 2006.

[2] Lambot S., Slob E.C., Vanclooster M. and Vereecken H. “Closed loop GPR data inversion for soil hydraulic and electric property determination.” *Geophysical ResearchLetter*, vol. 33, L21450, pp. 1-5, 2006.

[3] Luong M.P. “Introducing infrared thermography in soil dynamics.” *Infrared Physics & Technology*, vol. 49, pp. 306-311, 2007.

[4] Bouten W., Heuvelink G.B.M., Huisman J.A. and Snepvangers J.J.J.C. “Mapping spatial variation in surface soil water content: comparison of ground penetrating radar and time domain reflectometry.” *Journal of Hydrology*, vol. 269, pp. 194-207, 2002.

[5] Muñoz J.D. and Kravchenko A. "Soil carbon mapping using on-the-go near infrared spectroscopy, topography and aerial photographs." *Geoderma*, vol. 166, pp. 102-110, 2011.

[6] Kodaira M. and Shibusawa S. "Using a mobile real-time soil visible-near infrared sensor for high resolution soil property mapping." *Geoderma*, vol. 199, pp. 64-79, 2013.

[7] Pozdnyakov A., Pozdnyakova L. and Zhang R. “Application of geophysical methodsto evaluate hydrology and soil properties in urban areas.” *Urban Water*, vol. 3, pp. 205-216, 2001.

[8] Bouma J., Heijs A.W.J., Lange J.D. and Schoute J.F.TH. "Computed tomography as a tool for non-destructive analysis of flow patterns in macroporous clay soils." *Geoderma*, vol. 64, pp.183-196, 1995.

[9] Garcia A., He Y., Hernandez A., Huang M. and Song H. “Prediction of soil macronutrients content using near-infrared spectroscopy.” *Computers and Electronics in Agriculture*, vol. 58, pp. 144-153, 2007.

[10] Or D. and Serbin G. “Ground-penetrating radar measurement of soil water content dynamics using a suspended horn antenna.” *IEEE Transactions on Gepscience and Remote Sensing*, vol. 42, pp. 1695-1705, 2004.

[11] Janik L.J.,McBratney A.B., Rossel R.A.V., Skjemstad J.O., and Walvoort D.J.J. “Visible, near infrared, mid infrared or combined diffuse reflectance spectroscopy for simultaneous assessment of various soil properties.” *Geoderma*, vol. 131, pp. 59-75, 2006.

[12] Noborio K.“ Measurement of soil water content and electrical conductivity by time domain reflectometry: a review.” *Computers and Electronics in Agriculture*, vol. 31, pp. 213-237, 2001.

[13] Igel J., Preetz H. and Takahashi K. "Electromagnetic soil properties and performance of GPR for landmine detection: How to measure, how to analyze and how to classify?" *Leibniz Institute for Applied Geophysics*, 2011.

[14] Osman S.B.A.B.S. and Siddiqui F. "Electrical Resistivity Based Non-Destructive Testing Method for Determination of Soil's Strength Properties." *Advanced Materials Research Vols*, pp. 1553-1557, 2012.

[15] Abidin M.H.B.Z., Ahmad F., Saad R. and Wijeyesekera D.C. "The Influence of Soil Moisture Content and Grain Size Characteristics on its Field Electrical Resistivity." *EJGE*, vol. 18, pp.699-705, 2013.

[16] Fallah-Safari M., Hafizi M.K. and Ghalandarzadeh A. "The relationship between clay geotechnical data and clay electrical resistivity." *Bollettino di Geofisica Teorica ed Applicata*, vol. 54, n.1, pp. 23-38, 2013.

[17] Allison H.D., Asmussen L.E., Perkins H.F. and Truman C.C. "Using ground penetrating radar to investigate variability in selected soil properties." *Journal of Soil and Water Conservation*, pp. 341-345, 1988.

[18] Collins M.E. and Doolittle J.A. "Use of soil information to determine application of ground penetrating radar." *Journal of Applied Geophysics*, vol. 33, pp. 101-108, 1995.

[19] Gehrels J.C., Overmeeren R.A. and Sariowan S.V. "Ground penetrating radar for determining volumetric soil water content; results of comparative measurements at two test sites." *Journal of Hydrology*, vol. 197, pp. 316-338, 1997.

[20] Hubbard S.S., Lunt I.A. and Rubin Y. "Soil moisture content estimation using ground-penetrating radar refection data." *Journal of Hydrology*, vol. 307, pp. 254-269, 2005.

[21] Cui Y.J., Delage P., Pereira J.M. and Muñoz-Castelblanco J.A. "The influence of changes in water content on the electrical resistivity of a natural unsaturated loess." *ASTM Geotechnical Testing Journal*, vol. 35, pp. 11-17, 2012.

[22] Anbazhagan p., Burman S. andChandran D. "Investigation of Soil Compaction Homogeneity in the Finished Building Using Ground Penetrating Radar." *ASCE*, pp. 773-782, 2013.

[23] Anbazhagan p., Chandran D., Dixit N.P.S. and Krishna M.A. "Investigation of soil saturation and compaction homogeneity in the failed soil nailed wall and fill using ground penetrating radar." *Fourth International Seminar on Forensic Geotechnical Engineering*, vol. 4, pp. 409-426, 2013.

[24] Das B.M. and Sobhan K. *Principles of Geotechnical Engineering.* Cengage Learning, 9th SI Edition, pp. 819, 2014.

Appendix A

Table 5: After 24 hours resistivity variations with water content for 1.5 x standard mold size using soil passing sieve No.16 using standard compaction

W%	**Vs(v)**	**VR_S (v)**	**VR_1 (v)**	**I (ma)**	**VR_S+VR_1 (v)**	**R_1x I (v)**	**Rs (Ω)**	**Resistivity (Ω.cm)**
6.708977	10.01	3.15	6.86	3.42	10.01	6.87	918.9	3912.47592
5.910852	10.01	3.35	6.66	3.32	10.01	6.67	1007.06	4287.841985
5.034441	10.01	3.76	6.25	3.115	10.01	6.25	1205.48	5132.671098
4.336266	10.01	4.35	5.66	2.82	10.01	5.66	1541.65	6564.009687
3.782355	10.01	4.88	5.13	2.56	10.01	5.14	1902.16	8098.982692
2.938932	10.01	5.82	4.19	2.09	10.01	4.2	2781.47	11842.89302
2.354001	10.01	6.74	3.27	1.63	10.01	3.27	4133.1	17597.83896
0	10.01	5.01	5	NA	10.01	NA	10080000	42918443

Table 6: After 24 hours resistivity variations with water content for 2 x standard mold size using soil passing sieve No.16 using standard compaction

W%	**Vs(v)**	**VR_S (v)**	**VR_1 (v)**	**I (ma)**	**VR_S+VR_1 (v)**	**R_1x I (v)**	**Rs (Ω)**	**Resistivity (Ω.cm)**
7.308519	10.01	3.61	6.4	3.19	10.01	6.41	1129.93	3540.55958
6.745011	10.01	3.72	6.29	3.13	10.01	6.29	1190.08	3729.035555
6.096124	10.01	3.95	6.06	3.02	10.01	6.06	1306.57	4094.049127
5.467728	10.01	4.24	5.77	2.88	10.01	5.78	1467.69	4598.907799
5.037413	10.01	4.5	5.51	2.75	10.01	5.52	1632	5113.762122
4.337298	10.01	5.02	4.99	2.49	10.01	6	2012.08	6304.717212
3.790867	10.01	5.52	4.49	2.24	10.01	4.5	2460.75	7710.594449
0	10.01	5.01	5	NA	10.01	NA	10080000	31585001.34

Table 7: Immediate resistivity variations with water content for soil passing sieve No.4 using standard compaction

W%	**Void Ratio (e)**	**Vs(v)**	**VR_S (v)**	**VR_1 (v)**	**I (ma)**	**VR_S+VR_1 (v)**	**R_1x I (v)**	**Rs (Ω)**	**Resistivity (Ω.cm)**
5.969121	0.847812	10	4.89	5.11	2.53	10	5.08	1944.57	12795.67626
4.211378	0.801232	10	6.3	3.7	1.85	10	3.71	3397.41	22355.66654
3.444217	0.780902	10	6.69	3.31	1.65	10	3.31	4052.61	26667.01923
3.036612	0.770101	10	7.13	2.87	1.43	10	2.87	4895	32210.12116
1.334123	0.724985	10	8.13	1.87	0.93	10	1.87	8744.69	57541.88445
0	0.689631	10	5	5	NA	10	NA	10070000	66262700.73

Table 8: After 24 hours resistivity variations with water content for soil passing sieve No.4 using standard compaction

W%	**Void Ratio (e)**	**Vs(v)**	**VR_S (v)**	**VR_1 (v)**	**I (ma)**	**VR_S+VR_1 (v)**	**R_1x I (v)**	**Rs (Ω)**	**Resistivity (Ω.cm)**
5.969121	0.847812	10	4.89	5.11	2.53	10	5.08	1944.57	12795.67626
4.136904	0.799259	10	5.69	4.31	2.14	10	4.3	2664.9	17535.59793
3.53871	0.783407	10	6.14	3.86	1.92	10	3.86	3200.33	21058.83903
3.14552	0.772987	9.99	6.68	3.31	1.65	10	3.31	4046.55	26627.14316
1.478266	0.728805	10	8.49	1.51	0.75	10	1.51	11325.33	74523.03401
0	0.689631	10	5	5	NA	10	NA	10070000	66262700.73

Table 9: Immediate resistivity variations with water content for soil passing sieve No.4 using heavy compaction

W%	**Void Ratio (e)**	**Vs(v)**	**VR_S (v)**	**VR_1 (v)**	**I (ma)**	**VR_S+VR_1 (v)**	**R_1x I (v)**	**Rs (Ω)**	**Resistivity (Ω.cm)**
6.156466	0.766233	10	4.48	5.52	2.75	10	5.52	1628.36	11015.36761
4.521667	0.722911	10	4.62	5.38	2.68	10	5.38	1723.34	11657.87886
3.559378	0.69741	10	5.36	4.64	2.31	10	4.64	2321	15700.86973
2.986066	0.682218	10	6.08	3.92	1.95	10	3.92	3120.21	21107.28597
0.775612	0.623641	10	9.16	0.84	0.42	10	0.84	21801.52	147480.752
0	0.603087	10	5	5	NA	10	NA	10070000	68120533.46

Table 10: After 24 hours resistivity variations with water content for soil passing sieve No.4 using heavy compaction

W%	Void Ratio (e)	Vs(v)	VR_S (v)	VR_1 (v)	I (ma)	VR_S+VR_1 (v)	R_1x I (v)	Rs (Ω)	Resistivity (Ω.cm)
6.156466	0.766233	10	4.48	5.52	2.75	10	5.52	1628.36	11015.36761
4.498235	0.72229	10	5.14	4.86	2.42	10	4.86	2124.23	14369.77962
3.680445	0.700619	10	5.59	4.41	2.2	10	4.42	2537.45	17165.08914
3.173525	0.687185	10	6.18	3.82	1.9	10	3.82	3255.16	22020.18229
0.913863	0.627304	10	9.06	0.94	0.47	10	0.94	19268.6	130346.307
0	0.603087	10	5	5	NA	10	NA	10070000	68120533.46

Table 11: Immediate resistivity variations with water content for soil passing sieve No.4 using light compaction

W%	Void Ratio (e)	Vs(v)	VR_S (v)	VR_1 (v)	I (ma)	VR_S+VR_1 (v)	R_1x I (v)	Rs (Ω)	Resistivity (Ω.cm)
7.247427	0.929351	10	4.86	5.14	2.56	10	5.14	1898.25	12490.881
6.316179	0.904672	10	5.26	4.74	2.36	10	4.74	2229.29	14669.19326
5.286126	0.877376	10	6.17	3.83	1.9	10	3.82	3255.16	21419.63187
4.620008	0.859724	10	6.73	3.27	1.63	10	3.27	4126.97	27156.32354
2.583779	0.805764	10	8.05	1.95	0.97	10	1.95	8301.28	54624.15415
0	0.737294	10	5	5	NA	10	NA	10070000	66262700.73

Table 12: After 24 hours resistivity variations with water content for soil passing sieve No.4 using light compaction

W%	Void Ratio (e)	Vs(v)	VR_S (v)	VR_1 (v)	I (ma)	VR_S+VR_1 (v)	R_1x I (v)	Rs (Ω)	Resistivity (Ω.cm)
7.247427	0.929351	10	4.86	5.14	2.56	10	5.14	1898.25	12490.881
6.243722	0.902752	10	5.31	4.69	2.34	10	4.7	2265.5	14907.46261
5.305064	0.877878	10	5.8	4.2	2.09	10	4.2	2776.69	18271.19945
4.703993	0.86195	10	6.32	3.68	1.83	10	3.67	3456.48	22744.35947
2.692466	0.808644	10	8.15	1.85	0.92	10	1.85	8861.57	58310.97924
0	0.737294	10	5	5	NA	10	NA	10070000	66262700.73

Table 13: Immediate resistivity variations with water content for soil passing sieve No.8 using standard compaction

W%	**Void Ratio (e)**	**Vs(v)**	**VR_S (v)**	**VR_1 (v)**	**I (ma)**	**VR_S+VR_1 (v)**	**R_1x I (v)**	**Rs (Ω)**	**Resistivity (Ω.cm)**
6.339597	0.811872	10.01	7.43	2.58	2.58	10.01	7.43	698.74	4597.854966
5.530884	0.790441	10.01	6.85	3.16	3.16	10.01	6.85	930.11	6120.317833
4.793848	0.770909	10.01	6.3	3.71	3.13	10.01	6.3	1184.08	7791.493414
4.130828	0.753339	10.01	6.18	3.83	3.07	10.01	6.18	1246.59	8202.822254
3.443655	0.735129	10.01	5.84	4.17	2.9	10.01	5.84	1437.72	9460.497527
2.501630	0.666262	10.01	5.22	4.79	2.38	10.01	4.79	2191.88	14423.02765
1.153509	0.557443	10.01	8.1	1.91	0.95	10.01	1.91	8522.84	56082.06517
0	0.643873	10	5	5	NA	10	NA	10070000	66262700.73

Table 14: Immediate resistivity variations with water content for soil passing sieve No.16 using standard compaction

W%	**Void Ratio (e)**	**Vs(v)**	**VR_S (v)**	**VR_1 (v)**	**I (ma)**	**VR_S+VR_1 (v)**	**R_1x I (v)**	**Rs (Ω)**	**Resistivity (Ω.cm)**
6.968084	0.752896	10	2.28	7.72	3.85	10	7.73	589.4	3878.374956
5.999614	0.727231	9.99	2.1	7.89	3.93	9.99	7.89	533.98	3513.699795
5.486019	0.713621	9.99	2.21	7.78	3.88	9.99	7.79	566.74	3729.267429
4.584442	0.689729	10.01	2.63	7.38	3.68	10.01	7.39	712.11	4685.832355
3.618944	0.664143	10.01	3.68	6.33	3.15	10.01	6.33	1169.78	7697.396431
2.862303	0.644092	9.99	3.95	6.04	3.01	9.99	6.04	1310.94	8626.258679
0	0.568241	10	5	5	NA	5	NA	10070000	66262700.73

Table 15: After 24 hours resistivity variations with water content for soil passing sieve No.16 using standard compaction

W%	**Void Ratio (e)**	**Vs(v)**	**VR_S (v)**	**VR_1 (v)**	**I (ma)**	**VR_S+VR_1 (v)**	**R_1x I (v)**	**Rs (Ω)**	**Resistivity (Ω.cm)**
6.726933	0.74297	10	2.28	7.72	3.85	10	7.73	589.4	3878.374956
5.858535	0.719957	10.01	2.61	7.4	3.69	10.01	7.41	704.74	4637.336218
5.333492	0.706043	10.01	2.83	7.18	3.58	10.01	7.19	788.09	5185.796606
4.410216	0.681577	10.01	3.28	6.73	3.35	10.01	6.73	980.09	6449.196659
3.499548	0.657444	10.01	4.08	5.93	2.95	10.01	5.92	1385.22	9115.036574
2.737938	0.637261	10.01	4.82	5.19	2.585	10.01	5.19	1864.34	12267.74612
0	0.564706	10	5	5	NA	10	NA	10070000	66262700.73

Table 16: Immediate resistivity variations with water content for soil passing sieve No.16 using heavy compaction

W%	**Void Ratio (e)**	**Vs(v)**	**VR_S (v)**	**VR_1 (v)**	**I (ma)**	**VR_S+VR_1 (v)**	**R_1x I (v)**	**Rs (Ω)**	**Resistivity (Ω.cm)**
6.887868	0.698199	10	2.32	7.68	3.83	10	7.69	602.97	4078.911426
6.006115	0.674833	9.99	1.77	8.22	4.1	9.99	8.23	428.59	2899.282963
5.16424	0.652523	9.99	2.22	7.78	3.89	10	7.81	560.12	3789.044012
4.103772	0.624421	10	2.9	7.14	3.585	10.04	7.2	781.4	5285.936926
3.066936	0.596945	10	3.78	6.22	3.1	10	6.22	1217.81	8238.119846
2.302602	0.57669	9.99	4.57	5.42	2.7	9.99	5.42	1692	11445.87315
0	0.515671	10	5	5	NA	10	NA	10070000	68120533.46

Table 17: After 24 hours resistivity variations with water content for soil passing sieve No.16 using heavy compaction

W%	Void Ratio (e)	Vs(v)	VR_S (v)	VR_1 (v)	I (ma)	VR_S+VR_1 (v)	R_1x I (v)	Rs (Ω)	Resistivity (Ω.cm)
6.679098	0.689707	10	2.32	7.68	3.83	10	7.69	602.97	4078.911426
5.836656	0.667382	10	2.58	7.42	3.7	10	7.43	694.7	4699.437398
4.99274	0.645018	10	2.96	7.04	3.51	10	7.05	841	5689.113072
3.918866	0.61656	10	3.73	6.27	3.12	10	6.26	1197.13	8098.225841
2.941545	0.590661	9.99	4.71	5.28	2.63	9.99	5.28	1790.48	12112.06085
2.170596	0.570231	10	5.73	4.27	2.13	10	4.28	2686.84	18175.66774
0	0.51271	10	5	5	NA	10	NA	10070000	68120533.46

Table 18: Immediate resistivity variations with water content for soil passing sieve No.16 using light compaction

W%	Void Ratio (e)	Vs(v)	VR_S (v)	VR_1 (v)	I (ma)	VR_S+VR_1 (v)	R_1x I (v)	Rs (Ω)	Resistivity (Ω.cm)
7.003643	0.849144	9.99	2.32	7.67	3.82	9.99	7.67	607.18	3995.371065
6.179731	0.82731	9.99	1.99	8	3.99	9.99	8.01	495.76	3262.204222
5.434663	0.807566	9.99	2.36	7.63	3.81	9.99	7.65	614.05	4040.577099
4.508255	0.783016	9.99	2.8	7.22	3.61	10.02	7.25	762.08	5014.645379
3.501427	0.756335	9.99	3.46	6.53	3.25	9.99	6.53	1065.85	7013.51535
2.71063	0.735379	9.99	4.23	5.76	2.87	9.99	5.76	1472.84	9691.594453
0	0.663547	10	5	5	NA	10	NA	10070000	66262700.73

Table 19: After 24 hours resistivity variations with water content for soil passing sieve No.16 using light compaction

W%	Void Ratio (e)	Vs(v)	VRs (v)	VR_1 (v)	I (ma)	VR_S+VR_1 (v)	R_1x I (v)	Rs (Ω)	Resistivity (Ω.cm)
6.767941	0.839233	9.99	2.32	7.67	3.82	9.99	7.67	607.18	3995.371065
6.03238	0.819741	10	2.56	7.44	3.7	10	7.43	694.7	4571.270923
5.281873	0.799852	10	2.89	7.11	3.54	10	7.11	816.86	5375.109207
4.351212	0.77519	10	3.43	6.57	3.275	10	6.58	1045.44	6879.213292
3.371777	0.749235	10	4.33	5.66	2.82	9.99	5.66	1538.1	10121.01887
2.570921	0.728012	10	5.3	4.7	2.34	10	4.7	2265.5	14907.46261
0	0.659883	10	5	5	NA	10	NA	10070000	66262700.73

Table 20: Immediate resistivity variations with water content for soil passing sieve No.50 using standard compaction

W%	Void Ratio (e)	Vs(v)	VRs (v)	VR_1 (v)	I (ma)	VR_S+VR_1 (v)	R_1x I (v)	Rs (Ω)	Resistivity (Ω.cm)
7.433766	0.75629	10.02	1.77	8.26	4.13	10.03	8.29	418.15	2751.514231
6.539556	0.732594	10	2.4	7.6	3.81	10	7.65	616.67	4057.817245
5.267709	0.698889	10.01	3.25	6.66	3.32	10.01	6.67	1007.06	6626.664885
4.624025	0.681832	10	4.58	5.42	2.7	10	5.42	1695.7	11158.05974
0	0.559294	10	5	5	NA	10	NA	10070000	66262700.73

Table 21: After 24 hours resistivity variations with water content for soil passing sieve No.50 using standard compaction

W%	Void Ratio (e)	Vs(v)	VRs (v)	VR_1 (v)	I (ma)	VR_S+VR_1 (v)	R_1x I (v)	Rs (Ω)	Resistivity (Ω.cm)
7.47964	0.757505	10	2.66	7.34	3.66	10	7.35	724.24	4765.650286
6.629765	0.734983	10.01	4.05	6.96	3.46	10.01	6.95	885.06	5823.879435
5.425159	0.703061	10	4.82	5.18	2.58	10	5.18	1867.97	12291.63228
4.94849	0.690429	10	5	5	2.49	10	5	2008.06	13213.45371
0	0.559294	10	5	5	NA	10	NA	10070000	66262700.73

Table 22: Immediate resistivity variations with water content for soil passing sieve No.50 using heavy compaction

W%	Void Ratio (e)	Vs(v)	VR_S (v)	VR_1 (v)	I (ma)	VR_S+VR_1 (v)	R_1x I (v)	Rs (Ω)	Resistivity (Ω.cm)
7.130298	0.771716	10	1.05	8.95	4.46	10	8.96	234.15	1583.954609
6.22725	0.747785	10	1.56	8.44	4.21	10	8.45	367.3	2484.674473
4.66022	0.706259	10	2.1	7.9	3.94	10	7.91	530.07	3585.764764
3.945339	0.687314	10	2.21	7.79	3.88	10	7.79	569.32	3851.279256
0	0.582763	10	5	5	NA	10	NA	10070000	68120533.46

Table 23: After 24 hours resistivity variations with water content for soil passing sieve No.50 using heavy compaction

W%	Void Ratio (e)	Vs(v)	VR_S (v)	VR_1 (v)	I (ma)	VR_S+VR_1 (v)	R_1x I (v)	Rs (Ω)	Resistivity (Ω.cm)
7.274508	0.775537	10	1.63	8.37	4.17	10	8.37	390.08	2638.774349
6.359893	0.7513	10	2	8	3.98	10	7.99	504.56	3413.197255
4.901598	0.712655	10	3.11	6.89	3.42	10	6.89	915.98	6196.330312
4.364088	0.698411	10	3.28	6.72	3.35	10	6.73	977.07	6609.585862
0	0.582763	10	5	5	NA	10	NA	10070000	68120533.46

Table 24: Immediate resistivity variations with water content for soil passing sieve No.50 using light compaction

W%	Void Ratio (e)	Vs(v)	VR_S (v)	VR_1 (v)	I (ma)	VR_S+VR_1 (v)	R_1x I (v)	Rs (Ω)	Resistivity (Ω.cm)
8.35196	0.93006	10.01	2.46	7.56	3.78	10.02	7.59	640.15	4212.320543
7.053774	0.895658	10	2.58	7.42	3.72	10	7.47	680.17	4475.660492
5.270489	0.848401	10	4.01	5.99	2.98	10	5.98	1347.7	8868.147147
4.452543	0.826725	10	5.38	4.62	2.3	10	4.62	2339.83	15396.56952
0	0.708733	10	5	5	NA	10	NA	10070000	66262700.73

Table 25: After 24 hours resistivity variations with water content for soil passing sieve No.50 using light compaction

W%	**Void Ratio (e)**	**Vs(v)**	**VR_S (v)**	**VR_1 (v)**	**I (ma)**	**VR_S+VR_1 (v)**	**R_1x I (v)**	**Rs (Ω)**	**Resistivity (Ω.cm)**
8.398121	0.931283	10	2.72	7.28	3.63	10	7.29	746.82	4914.231396
6.980888	0.893726	10	3.13	6.87	3.42	10	6.87	915.98	6027.339485
5.442177	0.85295	10	5.66	4.34	2.16	10	4.34	2621.63	17250.87231
4.747328	0.834537	10	6.94	3.06	1.52	10	3.05	4570.95	30077.80456
0	0.708733	10	5	5	NA	10	NA	10070000	66262700.73

Table 26: Effect of 10% clay content on resistivity for soil passing sieve No.16 using standard compaction

W%	**Vs(v)**	**VR_S (v)**	**VR_1 (v)**	**I (ma)**	**VR_S+VR_1 (v)**	**R_1x I (v)**	**Rs (Ω)**	**Resistivity (Ω.cm)**
10.72409	10	2.81	7.19	3.6	10	7.23	769.78	5065.312986
7.598245	10	3.8	6.2	3.09	10	6.2	1228.25	8082.141228
7.074837	10	4.1	5.9	2.94	10	5.9	1393.36	9168.599472
6.49686	10	4.94	5.06	2.52	10	5.06	1960.25	12898.85393
5.829727	9.99	5	4.99	2.49	9.99	5	2004.05	13187.06707
5.245602	10	5.81	4.19	2.08	10	4.18	2799.69	18422.54425
0	10	4.99	5.01	NA	10	NA	10050000	66131096.56

Table 27: Effect of 20% clay content on resistivity for soil passing sieve No.16 using standard compaction

W%	**Vs(v)**	**VR_S (v)**	**VR_1 (v)**	**I (ma)**	**VR_S+VR_1 (v)**	**R_1x I (v)**	**Rs (Ω)**	**Resistivity (Ω.cm)**
13.18082	10	3.72	6.28	3.13	10	6.29	1186.89	7809.9838
10.57746	10	4.42	5.58	2.79	10	5.6	1576.23	10371.92222
9.707764	10	5.2	4.8	2.39	10	4.8	2176.1	14319.19196
8.81849	10	5.64	4.36	2.17	10	4.36	2600.29	17110.45065
7.820709	9.99	5.72	4.27	2.13	9.99	4.28	2682.14	17649.04073
7.026074	10	6.08	3.92	1.95	10	3.92	3120.21	20531.63272
0	10	5	5	NA	10	NA	10070000	66262700.73

Table 28: Effect of 30% clay content on resistivity for soil passing sieve No.16 using standard compaction

W%	**Vs(v)**	**VR_S (v)**	**VR_1 (v)**	**I (ma)**	**VR_S+VR_1 (v)**	**R_1x I (v)**	**Rs (Ω)**	**Resistivity (Ω.cm)**
12.55215	10	3.39	6.61	3.29	10	6.61	1031.51	6787.550986
10.59894	10	3.78	6.22	3.1	10	6.22	1217.81	8013.443851
9.785033	10	4.5	5.5	2.74	10	5.5	1641.64	10802.33367
8.832319	10	5.08	4.92	2.45	10	4.92	2073.63	13644.91799
8.181501	9.99	5.89	4.1	2.04	9.99	4.1	2889.06	19010.61749
7.52158	10	7.5	2.5	1.24	10	2.49	6056.52	39853.16507
0	10	4.96	5.04	NA	10	NA	9910000	65209867.35

Appendix B

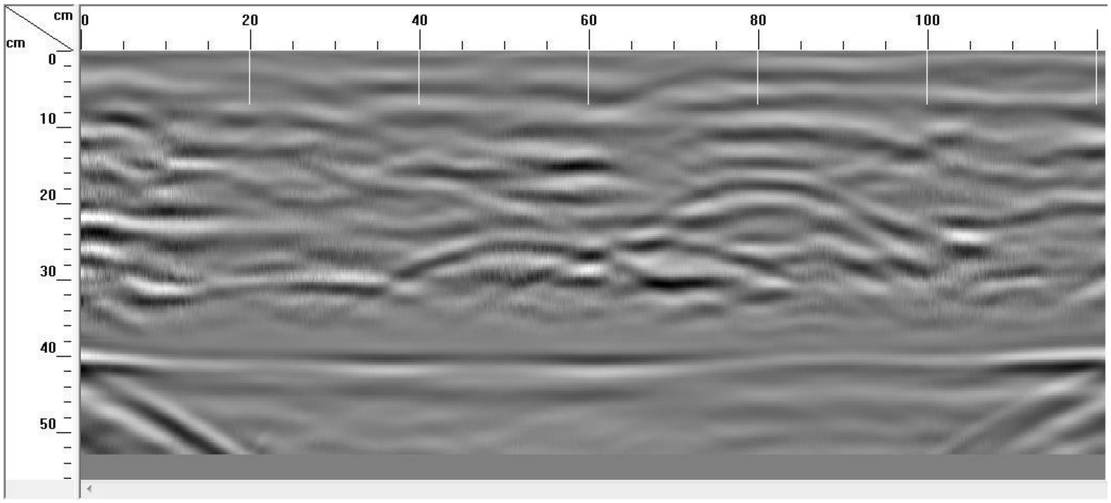

Figure 41: Water content 0.00 %, with compaction, dielectric constant 4.0

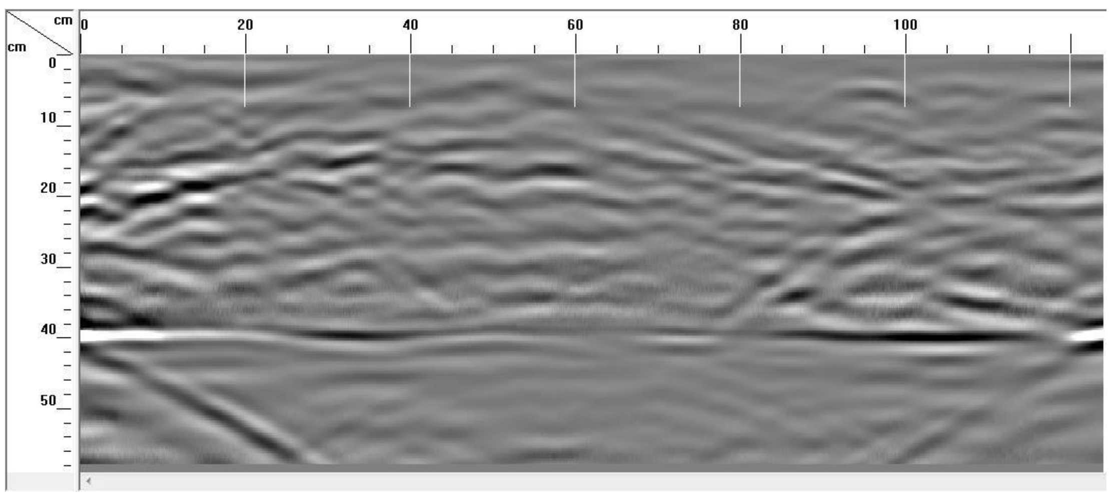

Figure 42: Water content 2.01 %, with compaction, dielectric constant 5.2

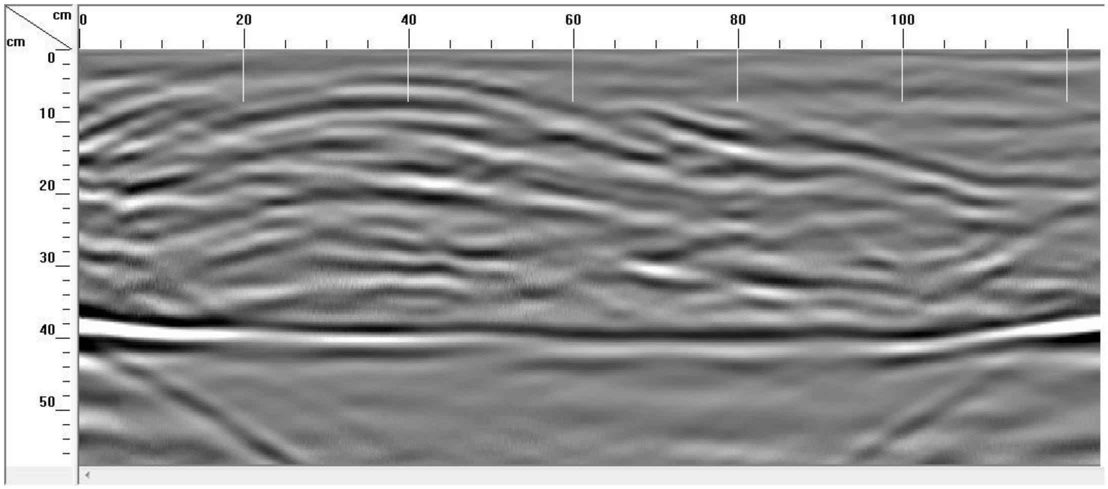

Figure 43: Water content 4.29 %, with compaction, dielectric constant 7.2

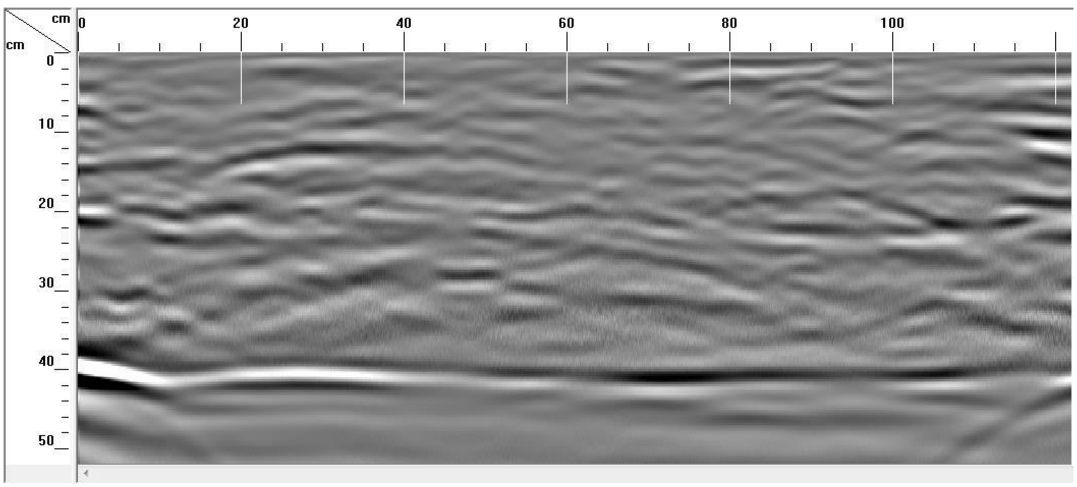

Figure 44: Water content 8.22 %, with compaction, dielectric constant 10.5

Appendix C

Table 31: Variations of friction angle with different water contents

Soil Used	Water Content %	Friction Angle (ϕ)
RAK Soil Passing Sieve No. 4	0	55^0
	3.46	43^0
	5.81	40^0
RAK Soil Passing Sieve No. 8	0	52^0
	3.86	39^0
	7.04	40^0
RAK Soil Passing Sieve No. 16	0	46^0
	4.14	35^0
	6.73	31^0
RAK Soil Passing Sieve No. 50	0	38^0
	4.28	31^0
	7.53	30^0

Vita

Fateh Tamam Alkej was raised in the city of Abu Dhabi, in the United Arab Emirates. He was educated in Al Dhafra Private School where he received his high school degree in 2010. After getting his high school degree, Fateh moved to the city of Sharjah in which he continued his studies at the American University of Sharjah and got his Bachelor's degree in Civil Engineering in 2014. After graduating, Fateh received a graduate studying scholarship to continue his higher studies in order to get a Master's degree in the Science of Engineering.